Published in final edited form as:

Anat Rec (Hoboken). 2022 September ; 305(9): 2175–2206. doi:10.1002/ar.24870.

Craniofacial growth and morphology among intersecting clinical categories

Ryan P. Knigge[1,2,3], **Anna M. Hardin**[2,4], **Kevin M. Middleton**[2], **Kieran P. McNulty**[5], **Heesoo Oh**[6], **Manish Valiathan**[7], **Dana L. Duren**[2,3], **Richard J. Sherwood**[2,3,7]

[1]Department of Integrative Biology and Physiology, University of Minnesota Medical School, Minneapolis, MN, 55455

[2]Department of Pathology and Anatomical Sciences, University of Missouri School of Medicine, Columbia, MO 65201

[3]Department of Orthopaedic Surgery, University of Missouri School of Medicine, Columbia, MO 65201

[4]Department of Biology, Western Oregon University, Monmouth, OR, 97361

[5]Department of Anthropology, University of Minnesota, Minneapolis, MN, 55455

[6]Department of Orthodontics, Arthur A. Dugoni School of Dentistry, University of the Pacific, San Francisco, CA

[7]Department of Orthodontics, School of Dental Medicine, Case Western Reserve University, Cleveland, OH

Abstract

Differential patterns of craniofacial growth are important sources of variation that can result in skeletal malocclusion. Understanding the timing of growth milestones and morphological change associated with adult skeletal malocclusions is critical for developing individualized orthodontic growth modification strategies. To identify patterns in the timing and geometry of growth, we used Bayesian modeling of cephalometrics and geometric morphometric analyses with a dense, longitudinal sample consisting of 15,407 cephalograms from 1,913 individuals between 2 and 31 years of age. Individuals were classified into vertical facial types (hyper-, normo-, hypo-divergent) and anteroposterior (A-P) skeletal classes (Class I, Class II, Class III) based on adult mandibular plane angle and ANB angle, respectively. These classifications yielded eight facial type-skeletal class categories with sufficient sample sizes to be included in the study. Four linear cephalometrics representing facial heights and maxillary and mandibular lengths were fit to standard double logistic model generating type-class category-specific estimates for age, size, and rate of growth at growth milestones. Mean landmark configurations were compared among type-class categories at four time points between 6 and 20 years of age. Overall, morphology and growth patterns were more similar within vertical facial types than within A-P classes and variation among A-P classes typically nested within variation among vertical types. Further, type-class-associated variation in

Corresponding author: Richard J. Sherwood, Dept. of Pathology and Anatomical Sciences, School of Medicine, University of Missouri, M263 Medical Science Building, One Hospital Dr., Columbia, MO 65212, (573) 882-6174, sherwoodrj@missouri.edu.

the rate and magnitude of growth in specific regions identified here may serve as targets for clinical treatment of complex vertical and A-P skeletal malocclusion and provide a clearer picture of the development of variation in craniofacial form.

Keywords

craniofacial growth; growth modeling; malocclusion; geometric morphometrics; cephalometrics

INTRODUCTION

The human craniofacial complex is often described as consisting of multiple modular regions or units, suggesting that there is strong integration within a region but weak integration among regions (Klingenberg, 2013). Some studies have considered larger divisions of the cranial vault, cranial base, and face as separate modules (Bastir & Rosas, 2006; Bookstein et al., 2003; Cheverud, 1995; Gkantidis & Halazonetis, 2011; Makedonska et al., 2012; Marroig et al., 2003; Singh et al., 2012), whereas others have divided the craniofacial complex into smaller structural or functional units (Cheverud, 1982, 1995; Goswami, 2006b, 2006a; Gunz & Harvati, 2007; Harvati et al., 2011; Makedonska et al., 2012; Marroig et al., 2003).

Regardless of how they are divided, units of the craniofacial complex are considered to have some degree of autonomy, but must also coordinate growth of tissues across the lifespan to maintain functional efficiency. For example, Enlow et al. (1969) suggested that anterior and posterior regions of the face, divided at the posterior maxillary (PM) plane, are separate but interacting modules. The positions of these regions are influenced by different structures, with the anterior face dependent upon the length of the anterior cranial base and the posterior face associated with the position of the middle cranial fossa and lateral cranial base (Bastir et al., 2004; Bastir & Rosas, 2005). Nevertheless, postnatal growth of the posterior and anterior face must be coordinated to maintain respiratory and masticatory function at all stages of growth. For example, the mandibular ramus of the posterior face bridges the pharyngeal space to facilitate occlusion of the upper and lower dentition in the anterior face (Bhat & Enlow, 1985; Enlow et al., 1982; Enlow & Hans, 1996).

With multiple interacting units in the craniofacial complex, a lack of coordinated growth can manifest in the misalignment of structures with lasting aesthetic and functional outcomes that may require clinical intervention such as orthodontic treatment or orthognathic surgery. In order to treat discordant growth among craniofacial components, clinicians must be able to accurately assess a patient's current anatomy, estimate future growth, and have an understanding of how a particular treatment strategy will affect an individual's growth to achieve a positive outcome.

Classification of craniofacial morphology

Clinicians often rely on classification systems to describe and diagnose patterns of craniofacial morphology, particularly how they deviate from what are considered ideal dental and skeletal relationships. The craniofacial variation these systems describe can manifest from differential growth processes. Clinicians can use patterns of morphology and growth associated with classifications to develop optimal treatment plans (Proffit, 2019). For example, Angle classification is used in orthodontics to diagnose, and determine appropriate treatment of, dental malocclusion based on maxillary and mandibular dental relationships (Ackerman & Proffit, 1969; Angle, 1899).

Classification systems describing vertical and/or anteroposterior (A-P) disharmony of the facial skeleton are often based on linear and angular cephalometric measurements (e.g., Björk, 1966; Greenstein, 1943; Jacobson, 1975). Of particular importance are: 1) Steiner's analysis (Proffit et al., 2019; Steiner, 1953) which defines A-P relationships of the maxilla and mandible based on the ANB angle (Point A-Nasion-Point B) and 2) Schudy's (1964) classification of vertical skeletal divergence which defines vertical relationships of the anterior and posterior face based on mandibular plane angle (angle between Sella-Nasion and Gonion-Menton planes). A-P relationships are typically described as Class I, II, or III, with Class I referring to a neutral maxillary and mandibular relationship, Class II referring to an anteriorly positioned maxilla relative to the mandible, and Class III referring to a posteriorly positioned maxilla relative to the mandible. Vertical skeletal divergence is often described as hyper-, normo-, or hypo-divergent, where hyper-divergent refers to a tall anterior face relative to the posterior facial height, normo-divergent refers to a neutral relationship between the anterior and posterior facial heights, and hypo-divergent refers to a short anterior face relative to the posterior facial height. These two classifications of vertical skeletal divergence and A-P skeletal malocclusion, and the associated patterns of craniofacial growth and development, are the primary focus of this study.

Previous studies of growth among different craniofacial classifications

Numerous studies have described differences in craniofacial growth associated with different classification categories by comparing growth in one or more types of malocclusion (skeletal or dental) to growth in a control group. Most studies comparing categories of vertical skeletal divergence identify differences in morphology among groups early in childhood, by approximately 5 or 6 years of age (e.g., Bishara & Jakobsen, 1985; Hardin et al., 2020; Moon et al., 2013; Nanda, 1988; Oh et al., 2019). Although Bishara and Jakobsen (1985) found parallel growth trajectories in dental and craniofacial cephalometrics among classification groups during adolescence, numerous other studies identified differences in adolescent craniofacial growth in relation to mandibular rotation (Björk, 1969; Björk & Skieller, 1983; Karlsen, 1995, 1997), vertical facial growth (Hardin et al., 2020; Jacob & Buschang, 2011), mandibular growth (Buschang et al., 2002; Oh et al., 2019), and the overall morphological pattern of the facial skeleton (Knigge et al., 2021).

When considering growth associated with different A-P categories, classification systems are based on dental (e.g., Angle classification) and/or skeletal (e.g., Steiner's analysis) relationships. Difficulties arise when comparing them as the two approaches often yield different findings. For example, some studies comparing craniofacial growth of individuals with Class II dental malocclusion to individuals without A-P dental malocclusion have found few if any significant differences in growth of the facial skeleton (Bishara, 1998; Rothstein & Yoon-Tarlie, 2000). This is because dental malocclusion can result from differences in skeletal growth or can be a manifestation of dental positioning only (Bishara, 2006).

Results from previous studies vary in identifying when differences in growth occur among A-P skeletal classification categories. For example, Riesmeijer et al. (2004) found differences between Class I and Class II individuals in mandibular length in 8- to 11-year-olds but not at older ages. In contrast, other studies have found deficient mandibular growth in Class II subjects during and after the adolescent growth spurt (Franchi et al., 2007; Stahl et al., 2008). Reyes et al. (2006) also found greater mandibular growth in Class III individuals compared to the control group during later stages of adolescence. Integrating these diverse findings is especially challenging because some studies do not describe whether dental or skeletal A-P malocclusion was used to classify individuals.

Fewer studies have compared morphology and growth across multiple vertical divergence and A-P malocclusion classes at the same time. Chung and Wong (2002) observed differences in mandibular rotation and facial convexity from ages 9 to 18 among vertical facial types within skeletal Class II individuals. Another study of hyper- and hypo-divergent individuals with dental Class II malocclusion found differences in the ratio of mandibular to maxillary volumes, but not in absolute mandibular or maxillary volumes (Nair et al., 2009). Vertical divergence and A-P malocclusion are expected to have interacting effects on the development of the craniofacial complex, and these impacts are often taken into account in orthodontic treatment (e.g., Buschang et al., 2002; Rogers et al., 2017) even if they have not yet been the focus of in-depth study. Thus, combined analysis of both vertical and A-P classification systems is needed to provide a holistic understanding of growth patterns and resulting morphological configurations.

Study goals

The aim of this study is to evaluate the morphology and timing of craniofacial growth that results in a misalignment of different regions of the face: anterior versus posterior face (i.e., vertical skeletal divergence) and maxilla versus mandible (i.e., A-P skeletal malocclusion). Our methodological approach unites traditional linear cephalometrics and geometric morphometrics: Bayesian longitudinal modeling of traditional linear cephalometrics allows for the precise estimation of growth parameters (e.g., magnitude, timing, and rates of growth) for linear dimensions of the craniofacial complex, whereas the application of the geometric morphometric toolkit provides a multivariate visualization of changes in the geometry and orientation of craniofacial structures. Together, these approaches enable us to address the following questions: 1) Do growth milestones (peak growth velocity and growth cessation) occur at different ages among divergence and malocclusion groups? 2) Does the rate of growth of linear cephalometrics differ among malocclusion groups? 3) Can specific regional differences in growth be identified for each malocclusion group, in comparison to the control group, that can potentially be targeted for clinical growth modification?

MATERIALS AND METHODS

CGCS Sample

The Craniofacial Growth Consortium Study (CGCS) consists of longitudinal landmark data collected from lateral cephalograms of participants in six North American growth studies between 1930 and 1982 (Sherwood et al., 2021; Tanner, 1981). Participants in these growth studies are predominantly of European ancestry. These studies were designed to characterize "healthy" growth. Treatment information is not available for the sample. Individuals with evidence of treatment (e.g., appliances) were excluded and it is clear few participants received treatment. Sherwood et al. (2021) provide details of the history of the CGCS, as well as cephalogram acquisition and digitization methods. The University of Missouri Institutional Review Board approved all procedures used in this study.

Cephalometric landmarks were digitized independently by three assessors in the software package eDigit, developed by the Craniofacial Research Instrumentation Laboratory (CRIL) at the University of the Pacific (Baumrind & Miller, 1980). Outlying landmarks were excluded based on established envelopes of error (Baumrind & Miller, 1980), and average values for the remaining landmarks were recorded for further analysis. The CGCS sample includes 15,407 digitized cephalograms from 1,913 individuals (956 females with 7,631 cephalograms, 957 males with 7,776 cephalograms) from 2 to 31 years of age. Inclusion criteria for each analysis are described below. The landmarks collected for this study are shown in Figure 1 with corresponding descriptions in Table 1.

Categorizing facial type and skeletal class

To determine vertical facial type and A-P skeletal class, respectively, mandibular plane angle (MPA) and ANB angle from all observations at ages 16 and older were averaged for each individual. MPA is the angle between the sella-nasion line and the gonion-menton plane. ANB is the angle between the nasion-point A and the nasion-point B lines. Only individuals with at least two observations over 16 years of age were included in this averaging and in the study. This averaging procedure ensures that an individual's facial type and class determination is based on their overall adult facial morphology, minimizing the effects of confounds like an open mouth or cranial rotation on facial type and class assessment. Facial type categorization was determined as: MPA greater than or equal to 39° indicates hyper-divergence, MPA greater than or equal to 28° and less than 39° indicates normo-divergence, and MPA less than 28° indicates hypo-divergence (Schudy, 1964, 1965); Skeletal class categorization was determined as: ANB greater than or equal to 4° indicates Class II, ANB greater than or equal to 0° and less than 4° indicates Class I, and ANB less than 0° indicates Class III (Proffit, 2019). Due to the small number of hyper-divergent Class III individuals in the sample (N=4, all male), hyper-divergent Class III individuals were excluded from further analyses. Sample sizes by facial type and skeletal class for subsequent analyses are provided in Table 2 and as a flowchart in Supplementary Figure 1. All Supplementary Information is available via NIH-figshare (https://figshare.com/s/b9c9968f3a6aafe75cb4).

Modeling linear measurements—For longitudinal modeling of linear craniofacial measurements, all individuals with a facial type-skeletal class categorization, as described above, were included in the sample. Double logistic models (Bock et al., 1973; Sherwood et al., 2021) were fit to four linear traits separately in males and females. The four cephalometrics were selected to capture antero-posterior growth of the maxilla (ANS-PNS) and mandible (Go-Pog), as well as vertical growth in the anterior face (N-Me) and posterior face (S-Go). The number of individuals and images evaluated for each trait and sex is provided (Supplementary Table 1). Trait value y is estimated in a standard double logistic model as follows:

$$y = \frac{a_1}{1 + e^{-b_1(age - c_1)}} + \frac{f - a_1}{1 + e^{-b_2(age - c_2)}}$$

where a_1 is the trait value at the first logistic asymptote, b_1 is the initial slope of the first logistic curve (considered the pre-pubertal component of the growth curve), c_1 is the age at initiation of the first logistic curve, b_2 is the initial slope of the second logistic curve (considered the pubertal component of the growth curve), c_2 is the age at maximum slope of the second logistic curve, and f is the trait value at the second logistic asymptote (considered the cessation of growth) (Supplementary Figure 2).

Fixed effects for facial type-skeletal class category and random effects for individual are included in the model as follows:

$$y = \frac{a_1 + a_{1TC}}{1 + e^{-1\left(b_1 + b_{1TC}\right)\left(age - c_1 + c_{1TC}\right)}} + \frac{(f + f_{TC}) - (a_1 + a_{1TC})}{1 + e^{-1\left(b_2 + b_{2TC}\right)\left(age - c_2 + c_{2TC}\right)}} + a_{TC} + a_{ID}$$

so that all parameters are free to vary by facial type-skeletal class category (TC) and the intercept (a) is free to vary by individual (ID). These models were fit to the data using the Hamiltonian Monte Carlo algorithm in the map2stan function from the package Rethinking, version 1.59 (McElreath, 2016). Starting values for primary parameters (a_1, b_1, c_1, b_2, c_2, f) were estimated from the data using Approximate Bayesian Computation (Supplementary Table 2). TC parameters were all sampled from normal distributions centered around zero with standard deviations of either 0.2 or 0.5 (Supplementary Table 2). ID parameters were sampled from normal distributions centered at 0 with variable standard deviations sampled from an exponential distribution.

Two growth parameters were estimated from the resulting models: peak growth velocity and growth cessation. Peak growth velocity is the local maximum of the rate of change at which acceleration is equal to zero. Age at peak growth velocity (aPGV), the mean, 5th percentile, and 95th percentile trait value at peak growth velocity (mean: sPGV), rate of growth at peak growth velocity (PGV), and the percentage of growth complete at peak growth velocity (gPGV) are estimated from posterior distributions. Growth cessation is defined as the age at which the model reaches 98% of the adult size asymptote (Hardin et al., 2021), equal to the sum of f, f_{TC}, and a_{TC}. Age at growth cessation (aGC), the mean, 5th percentile, and 95th percentile trait values at growth cessation (mean: sGC), growth rate at growth cessation (rGC), and the percentage of growth complete at growth cessation (gGC) were estimated from posterior distributions.

To assess differences between normo-divergent Class I growth (i.e., the control group) and that of other type-class groups (i.e., malocclusion groups), the distribution of the normo-divergent Class I model was subtracted from the distribution of each other type-class-specific model at one-year intervals from 6 to 20 years of age. The highest posterior density interval (HPDI) of the resulting distribution, representing the narrowest interval of the distribution that contains 90% of its samples, was then estimated. When the HPDI does not overlap with zero, the type-class model is considered significantly different from the normo-divergent Class I model at that age.

Geometric morphometric analysis—The full CGCS dataset was sampled to include only cephalograms with no missing landmark data and only individuals with at least one cephalogram taken within each of the following age ranges (or timepoints T1-T4) which maximize the available sample given that not every individual has a film at a given age: T1=6-8 years, T2=10-12 years, T3=14-16 years, and T4=18-20 years. When more than one cephalogram was available for an individual in a given age category, the cephalogram closest to the middle age for that category was selected (e.g., age 7 for T1), resulting in a total of four cephalograms per individual. The numbers of individuals for each facial category that meet these inclusion criteria are provided in Table 2 (Supplementary Figure 1).

The sets of 20 cranial landmarks and 18 mandibular landmarks were superimposed separately by generalized Procrustes analysis (Gower, 1975; Rohlf & Slice, 1990) without scaling, using the **Morpho** package in R (Schlager, 2017). The landmark configurations of the cranium and mandible were not scaled so as to retain variation in both size and shape (i.e., form) throughout the analysis. The resulting aligned cranial and mandibular coordinates were used as variables for subsequent analyses. The superimposition procedure and subsequent analyses were performed separately for males and females.

Mean configurations of the cranium and mandible were calculated for each type-class group, at each timepoint, and separately by sex. A principal component analysis (PCA) was performed on the mean configurations to visualize the mean cranial and mandibular growth trajectories for each type-class group. The mean landmark configurations for each type-class group are also figured separately relative to the normo-divergent Class I mean configuration at each time point, with 50% data ellipses around each landmark to illustrate differences in mandibular and cranial form with respect to the control group pattern.

RESULTS

Growth in the control sample: Normo-divergent, Class I

In normo-divergent Class I models, aPGV is between 11.1 and 11.8 years of age in females and between 12.3 and 14.3 years of age in males. Maxilla length (ANS-PNS) and posterior facial height (S-Go) reach PGV later than anterior facial height (N-Me) and mandible length (Go-Pog) in males and females. Posterior facial height has the most growth remaining at PGV for both females and males. Adolescent growth ceases between 14.3 and 19.2 years in females and between 16.3 and 20.2 years in males. For males and females, estimates of aGC increase from ANS-PNS to Go-Pog to N-Me to S-Go.

Double logistic growth curves, with HPDI plots, and landmark configurations for each type-class category are compared directly to the normo-divergent Class I results in Figures 2-15.

Comparison of each facial category to the control group

Hyper-divergent, Class I—Although morphological differences among hyper-divergent Class I and normo-divergent Class I females are present at age 6, (e.g., shorter posterior face, anteroposteriorly shorter maxilla and mandible, shorter mandibular ramus, and larger gonial angle), growth during adolescence magnifies many of these differences (Figure 2). Anterior facial height (N-Me) is similar at age 6, but hyper-divergent Class I females exhibit an increased rate and overall magnitude of growth of anterior facial height compared to normo-divergent Class I females (Figure 2A). This results from increases in the vertical dimensions of both the anterior upper face (N-ANS) and mandibular symphysis (Figure 2B). Posterior facial height (S-Go) exhibits less overall growth in hyper-divergent Class I females, resulting in a shorter posterior face at age 20 primarily resulting from less vertical growth of the mandibular ramus. The combined effects of increased growth of the anterior face and less growth of the posterior face results in a larger gonial angle in hyper-divergent Class I females compared to normo-divergent Class I females. Lastly, shorter maxillary (ANS-PNS) and mandibular (Go-Po) lengths are maintained in hyper-divergent Class I females compared to normo-divergent Class I females while exhibiting similar growth patterns.

Hyper-divergent Class I males differ from normo-divergent Class I males at age 6 by exhibiting a longer maxilla, a larger gonial angle, greater height of the anterior upper face, and taller mandibular symphysis (Figure 3). During adolescence, the hyper-divergent Class I maxilla exhibits much slower rates of anteroposterior maxillary growth resulting in a maxilla similar in length to that of normo-divergent Class I males by age 20 (Figure 3A). Anterior facial height in the hyper-divergent Class I group also exhibits a greater magnitude of PGV (Figure 3A) resulting from an increase in both mandibular symphyseal height and anterior upper facial height (Figure 3B). Greater vertical growth of the anterior face in the hyper-divergent Class I group combined with similar growth patterns in the posterior face correspond to a relatively larger gonial angle in the hyper-divergent Class I group. In both females and males, most variation in growth among these two classification groups appears to result primarily from differences in growth rate, rather than from differences in growth duration (Figures 2A and 3A).

Hyper-divergent, Class II—At age 6, hyper-divergent Class II females differ from normo-divergent Class I females by having a slightly longer maxilla (Figure 4). After 6 years of age, hyper-divergent Class II females maintain a longer maxilla and less A-P growth of the mandible (Figure 4A). Less A-P growth of the mandible in hyper-divergent Class II females results from slower overall growth rates during adolescence and an earlier cessation of adolescent growth. Furthermore, hyper-divergent Class II females exhibit greater vertical growth of the anterior face, resulting from increased growth of the anterior upper face and mandibular symphysis, and less growth in posterior facial height from less vertical growth of the mandibular ramus. These differences in the growth of anterior and posterior vertical dimensions result in a larger gonial angle in hyper-divergent Class II females compared to normo-divergent Class I females (Figure 4B).

Hyper-divergent Class II males are not substantially different from normo-divergent Class I males at 6 years of age (Figure 5). After age 6, hyper-divergent Class II males have slightly greater A-P growth of the maxilla and considerably less A-P growth of the mandible, resulting in a longer maxilla and shorter mandible at age 20 compared to normo-divergent Class I males (Figure 5A). Less A-P growth in the mandible appears to result from the absence of a peak in growth velocity in hyper-divergent Class II males. Hyper-divergent Class II males also exhibit less vertical growth of the mandibular ramus and increased growth of the anterior upper face and mandibular symphysis, as seen in females (Figure 5B). These differences in growth are associated with less vertical growth in the posterior face and greater growth in anterior facial height resulting in a larger gonial angle in hyper-divergent Class II males compared to normo-divergent Class I males.

Normo-divergent, Class II—Normo-divergent Class II females are very similar to normo-divergent Class I females at age 6 with no substantial differences in morphology (Figure 6). However, normo-divergent Class II females exhibit greater A-P growth of the maxilla after age 6, while maintaining similar proportions of mandibular length, anterior facial height, and posterior facial height resulting in a longer maxilla relative to both the length of the mandible and anterior cranial base.

Differences in craniofacial growth and morphology between normo-divergent Class I and Class II males are similar to those seen in females. Normo-divergent Class I and Class II males do not have any substantial differences in morphology at age 6, but normo-divergent Class II males exhibit greater A-P growth of the maxilla after age 6 (Figure 7). Other measurements maintain similar growth patterns between the two groups resulting in a relatively longer maxilla compared to both the mandible and anterior cranial base in the normo-divergent Class II group.

Normo-divergent, Class III—In both females and males, there are no substantial differences in morphology at age 6 between normo-divergent Class I and III groups (Figure 8 and 9). Normo-divergent Class III females have greater A-P growth of the mandible after age 6 compared to normo-divergent Class I females, with other measurements following similar growth patterns. This results in a longer mandible relative to the maxilla in normo-divergent Class III females at age 20. In addition, normo-divergent Class III females exhibit greater vertical growth of the mandibular ramus, but this does not correspond with a substantial increase in overall posterior facial height.

Similar to females, differences in morphology between normo-divergent Class I and III males at adulthood primarily result from growth differences after 6 years of age (Figure 9). Normo-divergent Class III males have a slower A-P maxillary growth rate and a faster A-P mandibular growth rate resulting in a shorter maxilla but longer mandible compared to adult normo-divergent Class I males at age 20.

Hypo-divergent, Class I—At age 6, hypo-divergent Class I females differ from normo-divergent Class I females by a vertically longer posterior face, due to a longer mandibular ramus, and a smaller gonial angle (Figure 10). After age 6, hypo-divergent Class I females exhibit higher rates of A-P maxillary and mandibular growth resulting in a longer maxilla and mandible. Hypo-divergent Class I females also have less vertical growth in the upper anterior face and mandibular symphysis, and greater vertical growth of the mandibular ramus compared to normo-divergent Class I females. The shorter anterior face and longer posterior face corresponds with a greater decrease in the gonial angle in hypo-divergent Class I females in comparison to the control group.

Hypo-divergent and normo-divergent Class I males differ at age 6 in having an anteroposteriorly longer mandible, a smaller gonial angle, a shorter anterior facial height, and a longer posterior facial height (Figure 11). After 6 years of age, a greater maxillary growth rate results in a longer maxilla while the anteroposteriorly longer mandible is maintained from age 6 onward. Posterior facial height is longer in the hypo-divergent Class I group resulting from greater growth of the mandibular ramus, and less vertical growth of the upper anterior face and mandibular symphysis results in a shorter anterior face. Together, these growth differences correspond with a greater decrease in gonial angle in hypo-divergent Class I males.

Hypo-divergent, Class II—Hypo-divergent Class II females have an anteroposteriorly longer maxilla, shorter anterior facial height, and longer posterior facial height and mandibular ramus than normo-divergent Class I females at age 6 (Figure 12). Hypo-divergent Class II females also exhibit faster rates of A-P maxillary and posterior facial height growth. The difference in posterior facial height growth is associated with an increase in ramus height. Although anterior facial height is greater at age 6 for hypo-divergent Class II females, substantially slower growth rates prior to PGV and an earlier cessation of growth result in a shorter anterior facial height in hypo-divergent Class II females by age 20. Less vertical growth in the face is observed in both the upper anterior face and the mandibular symphysis. Greater growth in the posterior cranial base is also observed in hypo-divergent females compared to the control group. Overall, these growth patterns are associated with a smaller gonial angle in hypo-divergent Class II females.

Hypo-divergent Class II males differ from normo-divergent Class I males at age 6 primarily by an anteroposteriorly longer maxilla and smaller anterior facial height (Figure 13). After 6 years of age, hypo-divergent Class II males exhibit faster rates of A-P maxillary growth and slower rates of vertical growth in the anterior face resulting in an even more elongated maxilla and a shorter anterior face at adulthood compared to normo-divergent Class I males. Hypo-divergent Class II males also exhibit increased growth of the posterior cranial base.

Hypo-divergent, Class III—At age 6, hypo-divergent Class III females differ from normo-divergent Class I females in having a longer mandibular ramus with a smaller gonial angle (Figure 14). Anterior facial height has a slower growth rate prior to aPGV, and posterior facial height exhibits faster growth after aPGV, resulting in a shorter anterior face and longer posterior face in adult hypo-divergent Class III females compared to normo-divergent Class I females. A shorter anterior face can be attributed to both a shorter upper anterior face and mandibular symphysis. Greater growth in the posterior face is associated with increased growth in ramus height and a greater decrease in the gonial angle. Hypo-divergent Class III females also exhibit a higher peak growth rate for mandibular length resulting in a relatively longer mandible.

Hypo-divergent Class III males only differ from normo-divergent Class I males at 6 years of age by a longer mandibular ramus and smaller gonial angle (Figure 15). Subsequent growth in hypo-divergent Class III males results in a shorter anterior face from less growth in the upper anterior face and mandibular symphysis, and a longer posterior face due to increased growth in ramus height and associated decrease in gonial angle. Hypo-divergent Class III males also exhibit faster mandibular A-P growth rates, resulting in a longer mandible compared to normo-divergent Class I males.

Multivariate growth trajectories

The principal component analyses of the mean mandibular and cranial landmark configurations of each type-class group, at each timepoint, provide a visualization of the multivariate growth trajectories for each group (Figures 16 and 17). Since the landmark configurations retain variation in size, the first principal component reflects differences in size as well as size correlated shape change and thus distributes the mean configurations of T1 through T4 from the negative to positive ends of the axis, respectively. The first principal components of the mandible and cranium PCAs account for 84.4% and 80.8% of the variation in females, respectively, and 88.5% and 87.6% of the variation in males, respectively. The second principal component consistently separates the hyper-divergent trajectories at the positive end from the hypo-divergent trajectories at the negative end with normo-divergent trajectories in-between for the cranium and mandible in both sexes. The second principal components of the mandible and cranium PCAs account for 9.2% and 10.4% of the variation in females, respectively, and 7.1% and 5.3% of the variation in males, respectively.

In females, mandibles of hyper-divergent individuals tend to be smaller on average and mandibles of hypo-divergent individuals tend to be larger on average at each timepoint. This pattern is evident by the negative shift of the hyper-divergent trajectories and positive shift of the hypo-divergent trajectories in the mandible PCA (Figure 16A). Within each vertical facial type, mandibles of Class II females are smaller and Class III females are larger on average. The female cranial trajectories do not indicate as much size variation among groups as observed among the mandible trajectories (Figure 16B). Within each vertical facial type, Class II crania are larger (in the hyper-divergent and normo-divergent groups) whereas Class III crania are smaller in comparison to Class I.

In males, the mandibular growth trajectories show less variation in size among vertical facial types relative to that observed in females (Figure 17A). However, Class II mandibles are smaller, and Class III mandibles are larger when compared to Class I mandibles within hyper- and hypo-divergent vertical facial type. There are no apparent differences in mandibular size among normo-divergent A-P skeletal classes. The cranial growth trajectories in males generally follow similar patterns except hyper-divergent Class I and normo-divergent Class II crania are larger on average at most timepoints compared to other groups (Figure 17B). Finally, both hyper-divergent Class I and II cranial growth trajectories show a distinct change in direction at T2 which is different from all other groups.

DISCUSSION

This study integrates analyses of traditional linear cephalometric measurements with landmark-based geometric morphometrics to provide a comprehensive understanding of differences in craniofacial growth and morphology among intersecting clinical categories of vertical facial divergence (i.e., vertical facial type) and A-P skeletal malocclusion (i.e., A-P skeletal class). It expands upon established knowledge of craniofacial growth by evaluating differences in the magnitude, timing, and duration of peak growth periods that result in different morphological categories of skeletal malocclusion in comparison to a control group. Furthermore, superimposition of the malocclusion and control group landmark configurations provides a unique visualization of how these growth differences are borne out in the size and shape of various facial components.

In order to determine optimal treatment for malocclusion within the craniofacial complex, it is necessary to understand those regions of the craniofacial complex which are misaligned and how misalignment manifests during growth and development. In this study, we categorized individuals *a priori* to either the control group (i.e., normo-divergent Class I) or to one of seven different clinical categories of skeletal malocclusion based on their adult morphology following established and commonly used criteria (Proffit et al., 2019). The growth exhibited by each malocclusion classification group and the overall morphology at various time points are compared to the control group to understand the growth processes leading to different types of craniofacial skeletal malocclusion.

Patterns of Growth and Morphology

Differences among classifications of vertical skeletal divergence reflect broader patterns of craniofacial disharmony across the craniofacial complex resulting in distinct morphological patterns in the cranium and mandible that are characteristic of each group. This is particularly evident in the geometric morphometric results by the overall degree of morphological similarity when comparing normo-divergent Class II and III to the control group and by the broader morphological differences when comparing hyper- and hypo-divergent Class I groups to the control group. This is also observed in the grouping of mandibular and cranial growth trajectories by vertical facial type rather than by A-P class. Generally, landmark configurations and characteristics of peak growth cessation tend to be most similar within vertical skeletal divergence classifications (i.e., hyper-, normo-, and hypo-divergent). Within the broader patterns (i.e., classifications of vertical skeletal divergence), individuals can be described as Class I, Class II, or Class III (i.e., A-P skeletal classifications) based on the A-P growth of the maxilla and mandible relative to each other. Furthermore, the nesting of A-P skeletal classifications within vertical skeletal divergence classifications reflects how similar A-P relationships of the maxilla and mandible can manifest from different growth processes depending on the pattern of vertical skeletal divergence. An important finding of this study was that a Class II maxillo-mandibular relationship is associated with less A-P growth of the mandible in the hyper-divergent group but greater A-P growth of the maxilla in the hypo-divergent group. This finding might suggest that growth modification by maxillary restriction is more effective in patients with a Class II, hypo-divergent malocclusion but may not be advisable for patients with a Class II, hyper-divergent malocclusion. An overview of the morphological patterns observed in each group are presented in Figure 18.

Although there is some variability in the specific morphological features previously reported for the three classifications of vertical skeletal divergence, likely resulting from differences in sample construction and classification method (e.g., Björk & Skieller, 1983; Enoki et al., 2004; Han & Park, 2019; Karlsen, 1997; Moon et al., 2013; Nanda, 1988), broader descriptions of morphological patterns are consistent across studies. In this study, hyper-divergent morphology is described by a longer upper anterior face and mandibular symphysis, shorter mandibular ramus, slightly shorter maxilla and mandible (in females), and a larger gonial angle in comparison to the control sample. The overall pattern of a tall anterior face and short posterior face results from growth that has been described as backwards mandibular rotation (Björk & Skieller, 1983) and also characterized as a coordinated pattern of growth and rotation of the maxilla and mandible when oriented on the anterior cranial base (Knigge et al., 2021). Conversely, hypo-divergent morphology is characterized by a shorter upper anterior face and mandibular symphysis, longer mandibular ramus, longer maxilla and mandible, and smaller gonial angle in comparison to the control group (Figure 18). The overall pattern of a short anterior face and long posterior face results from growth described as excessive forward rotation and relative elongation of the mandible (Björk & Skieller, 1983; Knigge et al., 2021). Previous descriptions of growth patterns for each vertical classification group in this sample are provided by Knigge et al., (2021).

After considering the overall facial pattern categorized by vertical skeletal divergence, A-P skeletal malocclusion can further result from uncoordinated growth of the maxilla and mandible. However, the growth patterns resulting in Class II or Class III malocclusion are not necessarily the same for each classification of vertical skeletal divergence (Figure 18). Class II malocclusion is achieved in normo-divergent and hypo-divergent groups primarily by excessive A-P maxillary growth in comparison to the control group. Mandibular length is also slightly shorter in the normo-divergent Class II group compared to the control group, but this difference is present at 6 years of age and similar mandibular growth is exhibited in both groups to adulthood. Conversely, Class II malocclusion in the hyper-divergent group results from restricted A-P mandibular growth with a relatively similar degree of maxillary growth compared to the control group. Some previous studies evaluating Class II craniofacial growth have suggested that A-P maxillomandibular discrepancies result primarily from restricted A-P mandibular growth with smaller increases in maxillary growth (Buschang & Martins, 1998; Jacob & Buschang, 2014; McNamara, 1981; Ngan et al., 1997; Stahl et al., 2008), whereas others have found excessive maxillary growth to be the primary contributor to skeletal Class II malocclusion (Riesmeijer et al., 2004). Restricted mandibular growth corresponds with the pattern observed in this study for the hyper-divergent Class II group, but excessive maxillary growth is seen in the normo-divergent and hypo-divergent Class II groups.

The observed patterns of growth in the Class III group in this study support previous analyses of Class III malocclusions. The negative ANB angle (i.e., protruded mandible relative to the maxilla) in Class III individuals results primarily from excessive A-P growth of the mandible with similar patterns of maxillary growth for both normo-divergent and hypo-divergent groups when compared to the control group (Figure 1). However, restricted A-P growth of the maxilla is also observed in normo-divergent Class III males. These observations are supported by previous analyses of Class III growth that have identified excessive mandibular growth as the main cause of Class III malocclusion (Baccetti et al., 2007; Battagel, 1993; Guyer et al., 1986; Reyes et al., 2006), with some also finding maxillary retrusion to be a contributing factor (Battagel, 1993; Guyer et al., 1986).

Timing of Growth and Treatment

Another important finding of this study is that the timings of peak growth velocity are generally similar between each classification of malocclusion and the control group, but peak growth velocity and age at growth cessation tend to vary. Thus, the timing of peak growth is similar, but the magnitude of growth velocity differs along with the length of the pubertal growth period. Table 3 summarizes the differences in the rate of peak growth and the ages at peak growth velocity and growth cessation between each malocclusion classification and the control group for each measurement (see Supplementary Table 3 for additional details). These results suggest that differences in initial morphology, growth rate, and duration of growth later in adolescence are all processes that can contribute to the development of these particular craniofacial skeletal misalignments. However, the timing of peak growth does not appear to substantially differ which may be significant for considering optimal growth modification strategies.

The results from our study do not agree with some prior work evaluating the timing and rate of growth associated with different craniofacial malocclusions. Aarts et al. (2015) found no difference in age at growth cessation between samples with short, average, and long facial types (i.e., hypo-divergent, normo-divergent, and hyper-divergent) based on linear measurements, including those analyzed here. Among the 16 comparisons between hyper-divergent Class I and hypo-divergent Class I with normo-divergent Class I (including all four measurements and both sexes), we found 5 instances where the difference in age at growth cessation was greater than six months. These conflicting results could stem from a number of differences in study design and, in particular, how growth cessation is estimated. Hardin et al. (2021) provides an assessment of how different methods and definitions of growth cessation can influence estimates of this milestone.

Previous studies have suggested that Class III individuals have a later age of peak mandibular growth and a later cessation of mandibular growth in comparison to Class I individuals (Battagel, 1993; Reyes et al., 2006). Reyes et al. (2006) found that peak growth in mandibular length for Class III individuals occurred between ages 11-12 years for females and ages 13-14 years for males. For both sexes, these estimates of peak growth occurred one year later than those observed in the control group (Reyes et al., 2006). Our results agree with an age of peak growth for mandibular length between 11 and 12 years of age for Class III females but also finds an earlier range of peak mandibular growth for Class III males between 12.3-12.8 years of age. Additionally, our estimates for peak mandibular growth in Class III individuals are not substantially different (i.e., > 6 months difference) from Class I individuals (Table 3 and Supplementary Table 3).

Since treatment strategies for many aspects of skeletal malocclusion focus on growth modification (Proffit et al., 2019), clinicians must be able to reasonably estimate the timing and amount of future growth. One of the benefits of longitudinal modeling is the ability to provide better estimates of growth milestones such as the age at peak growth velocity or age at cessation of growth. Our findings of a consistent age at peak growth velocity across categories of skeletal malocclusion but potential differences in growth rates and age at cessation of growth are important for identifying the appropriate timing for treatment through growth modification. Additionally, Heij et al. (2003, 2006) and Iseri and Solow (1996) have found that the timing of permanent tooth eruption varies by facial type. This variation in permanent tooth eruption does not appear to impact the timing of peak skeletal growth based on our analyses. However, the associated effects on overall skeletal morphology and other growth milestones among different facial types has not yet been tested in our sample, but would certainly be a factor when considering the optimal timing for treating dental malocclusions.

CONCLUSION

This study describes differences in craniofacial growth and morphology among different clinical classifications of skeletal malocclusion in comparison to a normo-divergent, Class I control group. A combination of longitudinal modeling of linear cephalometric measurements and a geometric morphometric analysis of cranial and mandibular form demonstrate that 1) the age at growth cessation, but not peak growth velocity, varies among type-class categories, 2) the rate of growth varies, especially among vertical facial type categories, and 3) growth of specific craniofacial regions vary more broadly among vertical facial types with A-P classes within each type varying by the anteroposterior growth of the maxilla and/or mandible.

The results of this study indicate that variation in initial morphology, growth rate, and timing of growth cessation are all factors that can contribute to differences in adult morphology representing skeletal misalignment. Vertical skeletal divergence results from broad differences in the growth of the craniofacial skeleton across multiple dimensions, whereas A-P skeletal classifications primarily reflect variation in A-P maxillomandibular growth. Considering the focus on growth modification for treating different classifications and combinations of skeletal malocclusion, the results of this study provide a comprehensive assessment of growth and morphology that can aid clinicians in identifying optimal approaches for treatment.

Supplementary Material

Refer to Web version on PubMed Central for supplementary material.

ACKNOWLEDGEMENTS

We are grateful to the long-term study participants who have made this work possible, as well as the many researchers who contributed to the studies that make up the Craniofacial Growth Consortium Study. Support for the CGCS was provided by the National Institute of Dental and Craniofacial Research (NIH) and the American Association of Orthodontists Foundation.

Grant sponsors:

National Institutes of Health, National Institute of Dental and Craniofacial Research, Grant/Award Numbers: R01 DE024732, R01 DE024732-06W1, F32 DE029104, R03 DE021435. American Association of Orthodontists Foundation, Grant/Award Number: Legacy Collection

REFERENCES

Aarts BE, Convens J, Bronkhorst EM, Kuijpers-Jagtman AM, & Fudalej PS (2015). Cessation of facial growth in subjects with short, average, and long facial types – Implications for the timing of implant placement. Journal of Cranio-Maxillofacial Surgery, 43(10), 2106–2111. 10.1016/j.jcms.2015.10.013 [PubMed: 26548528]

Ackerman JL, & Proffit WR (1969). The characteristics of malocclusion: A modern approach to classification and diagnosis. American Journal of Orthodontics, 56(5), 443–454. 10.1016/0002-9416(69)90206-1 [PubMed: 5261158]

Angle E (1899). Classification of malocclusion. Dental Cosmos, 41, 248–264.

Baccetti T, Franchi L, & McNamara JA (2007). Growth in the Untreated Class III Subject. Seminars in Orthodontics, 13(3), 130–142. 10.1053/j.sodo.2007.05.006

Bastir M, & Rosas A (2005). Hierarchical nature of morphological integration and modularity in the human posterior face. American Journal of Physical Anthropology, 128(1), 26–34. 10.1002/ajpa.20191 [PubMed: 15778978]

Bastir M, & Rosas A (2006). Correlated variation between the lateral basicranium and the face: A geometric morphometric study in different human groups. Archives of Oral Biology, 51(9), 814–824. 10.1016/j.archoralbio.2006.03.009 [PubMed: 16681992]

Bastir M, Rosas A, & Kuroe K (2004). Petrosal orientation and mandibular ramus breadth: Evidence for an integrated petroso-mandibular developmental unit. American Journal of Physical Anthropology, 123(4), 340–350. 10.1002/ajpa.10313 [PubMed: 15022362]

Battagel J (1993). The aetiological factors in Class III malocclusion. European Journal of Orthodontics, 15, 347–370. [PubMed: 8223970]

Baumrind S, & Miller DM (1980). Computer-aided head film analysis: The University of California San Francisco method. American Journal of Orthodontics, 78(1), 41–65. 10.1016/0002-9416(80)90039-1 [PubMed: 6930171]

Bhat M, & Enlow DH (1985). Facial Variations Related to Headform Type. Angle Orthodontist, 55(4), 269–280. [PubMed: 3865565]

Bishara SE (1998). Mandibular changes in persons with untreated and treated Class II Division 1 malocclusion. American Journal of Orthodontics and Dentofacial Orthopedics, 113(6), 661–673. 10.1016/S0889-5406(98)70227-6 [PubMed: 9637570]

Bishara SE (2006). Class II Malocclusions: Diagnostic and Clinical Considerations with and without Treatment. Seminars in Orthodontics, 12(1), 11–24. 10.1053/j.sodo.2005.10.005

Bishara SE, & Jakobsen JR (1985). Longitudinal changes in three normal facial types. American Journal of Orthodontics, 88(6), 466–502. 10.1016/S0002-9416(85)80046-4 [PubMed: 3878083]

Björk A (1966). Sutural Growth of the Upper Face Studied by The Implant Method. Acta Odontologica Scandinavica, 24(2), 109–127. 10.3109/00016356609026122 [PubMed: 5225742]

Björk A (1969). Prediction of mandibular growth rotation. American Journal of Orthodontics, 55(6), 585–599. 10.1016/0002-9416(69)90036-0 [PubMed: 5253957]

Björk A, & Skieller V (1983). Normal and abnormal growth of the mandible. A synthesis of longitudinal cephalometric implant studies over a period of 25 years. European Journal of Orthodontics, 5(1), 1–46. 10.1093/ejo/5.1.1 [PubMed: 6572593]

Bock RD, Wainer H, Petersen A, Thissen D, Murray J, Roche AA (1973). A parameterization for individual human growth curves. Human Biology, 45(1), 63–80. [PubMed: 4694175]

Bookstein FL, Gunz P, Mitteroecker P, Prossinger H, Schaefer K, & Seidler H (2003). Cranial integration in Homo: Singular warps analysis of the midsagittal plane in ontogeny and evolution. Journal of Human Evolution, 44, 167–187. [PubMed: 12662941]

Buschang P, & Martins J (1998). Childhood and adolescent changes of skeletal relationships. Angle Orthodontist, 3, 199–208.

Buschang P, Sankey W, & English JP (2002). Early treatment of hyperdivergent open-bite malocclusions. Seminars in Orthodontics, 8(3), 130–140. 10.1053/sodo.2002.125432

Cheverud JM (1982). Phenotypic, Genetic, and Environmental Morphological Integration in the Cranium. Evolution, 36(3), 499–516. 10.2307/2408096 [PubMed: 28568050]

Cheverud JM (1995). Morphological Integration in the Saddle-Back Tamarin (Saguinus fuscicollis) Cranium. The American Naturalist, 145(1), 63–89. 10.1086/285728

Chung C-H, & Wong WW (2002). Craniofacial growth in untreated skeletal Class II subjects: A longitudinal study. American Journal of Orthodontics and Dentofacial Orthopedics, 122(6), 619–626. 10.1067/mod.2002.129195 [PubMed: 12490873]

Enlow DH, & Hans MG (1996). Essentials of Facial Growth. Saunders.

Enlow DH, Moyers RE, Hunter WS, & McNamara JA (1969). A procedure for the analysis of intrinsic facial form and growth: An equivalent-balance concept. American Journal of Orthodontics, 56(1), 6–23. 10.1016/0002-9416(69)90254-1 [PubMed: 5255278]

Enlow D, Pfister C, Richardson E, & Kuroda T (1982). An analysis of Black and Caucasian craniofacial patterns. Angle Orthodontist, 52, 279–287. [PubMed: 6961829]

Enoki C, Telles C. de S., & Matsumoto MAN (2004). Dental-skeletal dimensions in growing individuals with variations in the lower facial height. Brazilian Dental Journal, 15(1), 68–74. 10.1590/S0103-64402004000100013 [PubMed: 15322649]

Franchi L, Baccetti T, Stahl F, & McNamara JA (2007). Thin-plate Spline Analysis of Craniofacial Growth in Class I and Class II Subjects. The Angle Orthodontist, 77(4), 595–601. 10.2319/070506-275 [PubMed: 17605492]

Gkantidis N, & Halazonetis DJ (2011). Morphological integration between the cranial base and the face in children and adults. Journal of Anatomy, 218(4), 426–438. 10.1111/j.1469-7580.2011.01346.x [PubMed: 21323666]

Goswami A (2006a). Cranial Modularity Shifts during Mammalian Evolution. The American Naturalist, 168(2), 270–280.

Goswami A (2006b). Morphological integration in the carnivoran skull. Evolution, 60(1), 169. 10.1554/05-110.1 [PubMed: 16568641]

Gower JC (1975). Generalized procrustes analysis. Psychometrika, 40(1), 33–51. 10.1007/BF02291478

Greenstein AV (1943). The tweed philosophy: An analysis. American Journal of Orthodontics and Oral Surgery, 29(9), 527–540. 10.1016/S0096-6347(43)90310-2

Gunz P, & Harvati K (2007). The Neanderthal “chignon”: Variation, integration, and homology. Journal of Human Evolution, 52(3), 262–274. 10.1016/j.jhevol.2006.08.010 [PubMed: 17097133]

Guyer E, Ellis E, McNamara J, & Behrents R (1986). Components of Class III Malocclusion in Juveniles and Adolescents. Angle Orthodontist, 7–30. [PubMed: 3485393]

Han SH, & Park Y (2019). Growth patterns and overbite depth indicators of long and short faces in Korean adolescents: Revisited through mixed-effects analysis. Orthodontics & Craniofacial Research. 10.1111/ocr.12255

Hardin A, Knigge R, Oh H, Valiathan M, Duren D, McNulty K, Middleton K, & Sherwood R (2021). Estimating Craniofacial Growth Cessation: Comparison of Asymptote- and Rate-based Methods. The Cleft Palate-Craniofacial Journal.

Hardin A, Valiathan M, Oh H, Knigge R, McNulty K, Leary E, Duren D, & Sherwood R (2020). Clinical Implications of Age-Related Change of the Mandibular Plane Angle. Orthodontics & Craniofacial Research, 23(1), 50–58. 10.1111/ocr.12342 [PubMed: 31465622]

Harvati K, Singh N, & López EN (2011). A Three-Dimensional Look at the Neanderthal Mandible. In Condemi S & Weniger G-C (Eds.), Continuity and Discontinuity in the Peopling of Europe (pp. 179–192). Springer Netherlands. 10.1007/978-94-007-0492-3_16

Heij DGO, Opdebeeck H, Steenberghe D, & Quirynen M (2003). Age as compromising factor for implant insertion. Periodontology 2000, 33(1), 172–184. 10.1046/j.0906-6713.2003.03314.x [PubMed: 12950850]

Heij DGO, Opdebeeck H, van Steenberghe D, Kokich VG, Belser U, & Quirynen M (2006). Facial development, continuous tooth eruption, and mesial drift as compromising factors for implant placement. The International Journal of Oral & Maxillofacial Implants, 21(6), 867–878. [PubMed: 17190296]

Iseri H, & Solow B (1996). Continued eruption of maxillary incisors and first molars in girls from 9 to 25 years, studied by the implant method. European Journal of Orthodontics, 18, 245–256. [PubMed: 8791889]

Jacob H, & Buschang P (2011). Vertical craniofacial growth changes in French-Canadians between 10 and 15 years of age. American Journal of Orthodontics and Dentofacial Orthopedics, 139(6), 797–805. 10.1016/j.ajodo.2010.02.032 [PubMed: 21640887]

Jacob H, & Buschang P (2014). Mandibular growth comparisons of Class I and Class II division 1 skeletofacial patterns. The Angle Orthodontist, 84(5), 755–761. 10.2319/100113-719.1 [PubMed: 24524578]

Jacobson A (1975). The “Wits” appraisal of jaw disharmony. American Journal of Orthodontics, 67(2), 125–138. 10.1016/0002-9416(75)90065-2 [PubMed: 1054214]

Karlsen AT (1995). Craniofacial growth differences between low and high MP-SN angle males: A longitudinal study. The Angle Orthodontist, 65(5), 341–350. 10.1043/0003-3219(1995)065<0341:CGDBLA>2.0.CO;2 [PubMed: 8526293]

Karlsen AT (1997). Association between facial height development and mandibular growth rotation in low and high MP-SN angle faces: A longitudinal study. The Angle Orthodontist, 67(2), 103–110. 10.1043/0003-3219(1997)067<0103:ABFHDA>2.3.CO;2 [PubMed: 9107374]

Klingenberg CP (2013). Cranial integration and modularity: Insights into evolution and development from morphometric data. Hystrix, the Italian Journal of Mammalogy, 24(1). 10.4404/hystrix-24.1-6367

Knigge R, McNulty K, Oh H, Hardin A, Leary E, Duren D, Valiathan M, & Sherwood R (2021). Geometric morphometric analysis of growth patterns among facial types. American Journal of Orthodontics and Dentofacial Orthopedics, 160(3), 430–441. [PubMed: 34175161]

Makedonska J, Wright BW, & Strait DS (2012). The Effect of Dietary Adaption on Cranial Morphological Integration in Capuchins (Order Primates, Genus Cebus). PLoS ONE, 7(10), e40398. 10.1371/journal.pone.0040398 [PubMed: 23110039]

Marroig G, Vivo M, & Cheverud JM (2003). Cranial evolution in sakis (Pithecia, Platyrrhini) II: Evolutionary processes and morphological integration: Cranial evolution in sakis. Journal of Evolutionary Biology, 17(1), 144–155. 10.1046/j.1420-9101.2003.00653.x

McElreath R (2016). Statistical Rethinking: A Bayesian Course with Examples in R and Stan. CRC Press.

McNamara J (1981). Components of Class II malocclusion in children 8-10 years of age. Angle Orthodontist, 51(3), 177–202. [PubMed: 7023290]

Moon S-C, Kim H-K, Kwon T-K, Han SH, An C-H, & Park Y-S (2013). Patterns of vertical facial growth in Korean adolescents analyzed with mixed-effects regression analysis. American Journal of Orthodontics and Dentofacial Orthopedics, 143(6), 810–818. 10.1016/j.ajodo.2013.01.016 [PubMed: 23726331]

Nair R, Deguchi TS, Li X, Katashiba S, & Chan YH (2009). Quantitative analysis of the maxilla and the mandible in hyper- and hypodivergent skeletal class II pattern. Orthodontics & Craniofacial Research, 12(1), 9–13. 10.1111/j.1601-6343.2008.01431.x [PubMed: 19154269]

Nanda SK (1988). Patterns of vertical growth in the face. American Journal of Orthodontics and Dentofacial Orthopedics, 93(2), 103–116. 10.1016/0889-5406(88)90287-9 [PubMed: 3422525]

Ngan PW, Byczek E, & Scheick J (1997). Longitudinal evaluation of growth changesin class II division 1 subjects. Seminars in Orthodontics, 3(4), 222–231. 10.1016/S1073-8746(97)80055-2 [PubMed: 9573884]

Oh H, Knigge R, Hardin A, Sherwood R, Duren D, Valiathan M, Leary E, & McNulty K (2019). Predicting adult facial type from mandibular landmark data at young ages. Orthodontics & Craniofacial Research, 22, 154–162. 10.1111/ocr.12296 [PubMed: 31074133]

Proffit W (2019). Concepts of growth and development. In Proffit W, Fields H, Larson B, & Sarver D (Eds.), Contemporary Orthodontics (6th Edition, pp. 18–59). Elsevier.

Proffit W, Fields H, Larson B, & Sarver D (2019). Contemporary Orthodontics (Sixth Edition). Elsevier.

Reyes BC, Baccetti T, & M. JA (2006). An Estimate of Craniofacial Growth in Class III Malocclusion. Angle Orthodontist, 76(4), 8.

Riesmeijer AM, Prahl-Andersen B, Mascarenhas AK, Joo BH, & Vig KWL (2004). A comparison of craniofacial Class I and Class II growth patterns. American Journal of Orthodontics and Dentofacial Orthopedics, 125(4), 463–471. 10.1016/j.ajodo.2003.05.012 [PubMed: 15067263]

Rogers K, Campbell P, Tadlock L, Schneiderman E, & Buschang P (2017). Treatment changes of hypo- and hyperdivergent Class II Herbst patients. The Angle Orthodontist, 88. 10.2319/060117-369.1

Rohlf FJ, & Slice D (1990). Extensions of the Procrustes Method for the Optimal Superimposition of Landmarks. Systematic Zoology, 39(1), 40. 10.2307/2992207

Rothstein T, & Yoon-Tarlie C (2000). Dental and facial skeletal characteristics and growth of males and females with Class II, Division 1 malocclusion between the ages of 10 and 14 (revisited)—Part I: Characteristics of size, form, and position. American Journal of Orthodontics and Dentofacial Orthopedics, 117(3), 320–332. 10.1016/S0889-5406(00)70237-X [PubMed: 10715092]

Schlager S (2017). Morpho and Rvcg—Shape Analysis in R. In Zheng G, Li S, & Szekely G (Eds.), Statistical Shape and Deformation Analysis (pp. 217–256). Academic Press.

Schudy F (1964). Vertical growth versus anteroposterior growth as related to function and treatment. Angle Orthodontist, 34, 75–93.

Schudy F (1965). The rotation of the mandible resulting from growth: Its implications in orthodontic treatment. Angle Orthodontist, 36, 36–50.

Sherwood RJ, Oh HS, Valiathan M, McNulty KP, Duren DL, Knigge RP, Hardin AM, Holzhauser CL, & Middleton KM (2021). Bayesian approach to longitudinal craniofacial growth: The Craniofacial Growth Consortium Study. The Anatomical Record, 304(5), 991–1019. 10.1002/ar.24520 [PubMed: 33015973]

Singh N, Harvati K, Hublin J-J, & Klingenberg CP (2012). Morphological evolution through integration: A quantitative study of cranial integration in Homo, Pan, Gorilla and Pongo. Journal of Human Evolution, 62(1), 155–164. 10.1016/j.jhevol.2011.11.006 [PubMed: 22178399]

Stahl F, Baccetti T, Franchi L, & McNamara JA (2008). Longitudinal growth changes in untreated subjects with Class II Division 1 malocclusion. American Journal of Orthodontics and Dentofacial Orthopedics, 134(1), 125–137. 10.1016/j.ajodo.2006.06.028 [PubMed: 18617112]

Steiner CC (1953). Cephalometrics for you and me. American Journal of Orthodontics, 39(10), 729–755. 10.1016/0002-9416(53)90082-7

Tanner JM (1981). A History of the Study of Human Growth. Cambridge University Press.

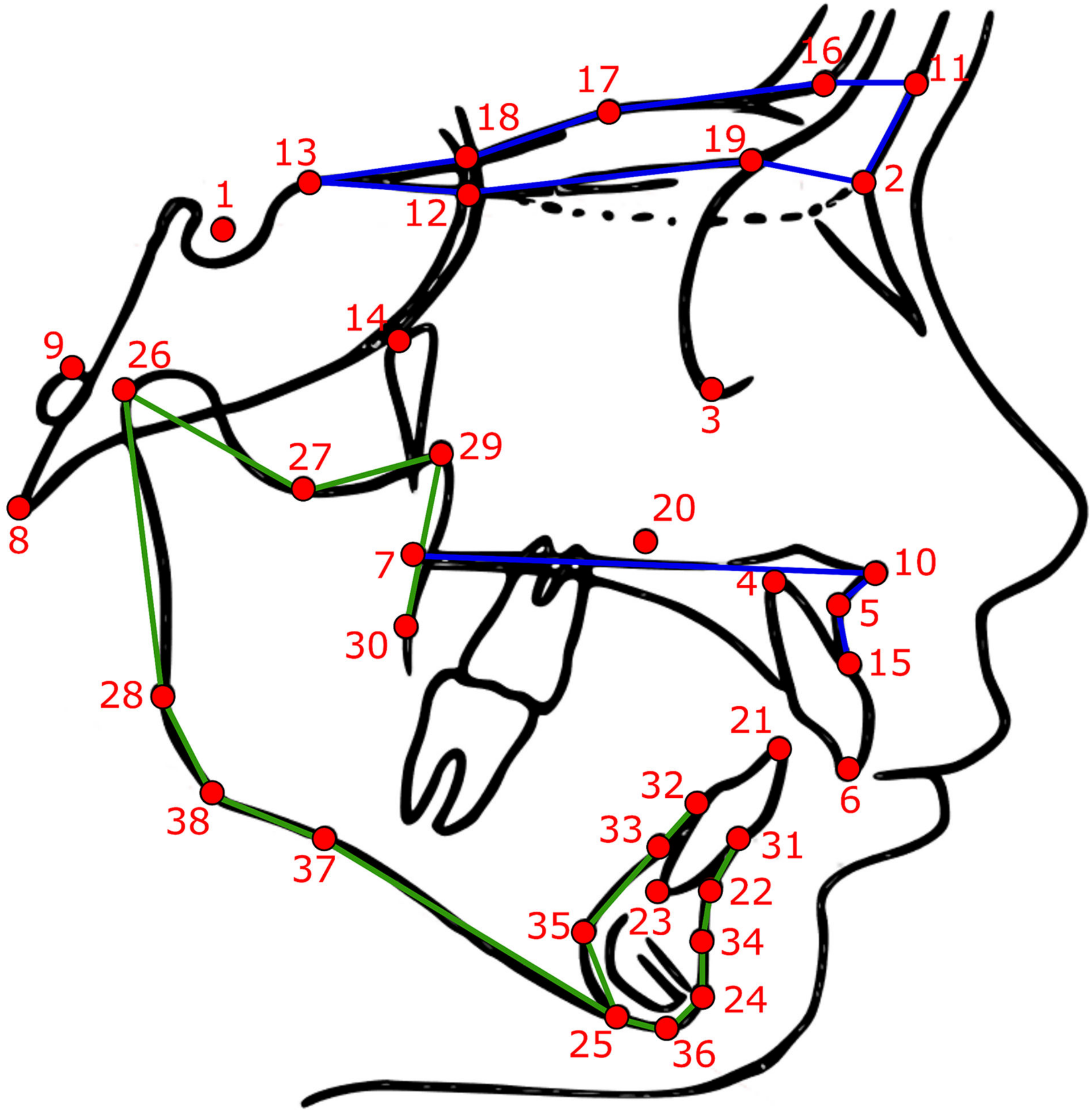

Figure 1:

Depiction of cephalometric landmarks used in this study. Modified from Sherwood et al., (2021). Landmark numbers correspond to descriptions in Table 1. Blue lines (cranium) and green lines (mandible) correspond to the wireframes shown in the Results figures.

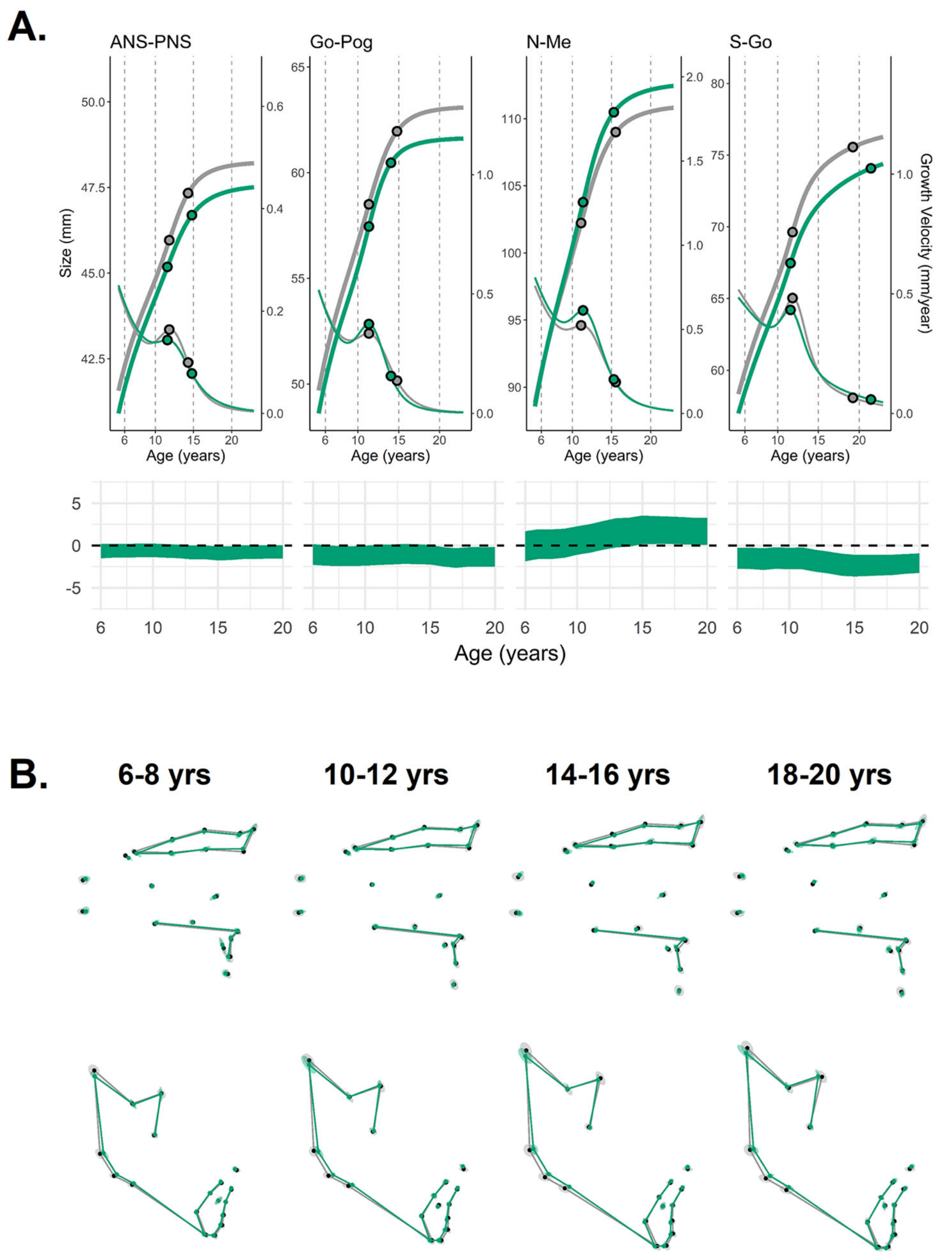

Figure 2:

Comparison of hyper-divergent Class I growth (solid green lines) to normo-divergent Class I growth (solid gray lines) in females. A: Plots for each of the four measurements with a double-logistic growth curve and velocity curve for each classification group. Circles indicate peak growth velocity and cessation of growth. Below each plot shows the HPDI comparing distribution values between classification groups. The dashed line at 0 represents no difference. The width of the band is the 90% HPDI of the difference between groups. When the dashed line falls outside of the band, the two groups are considered different at that age. B: Comparison of cranial and mandibular morphology between the two classification groups at the four timepoints.

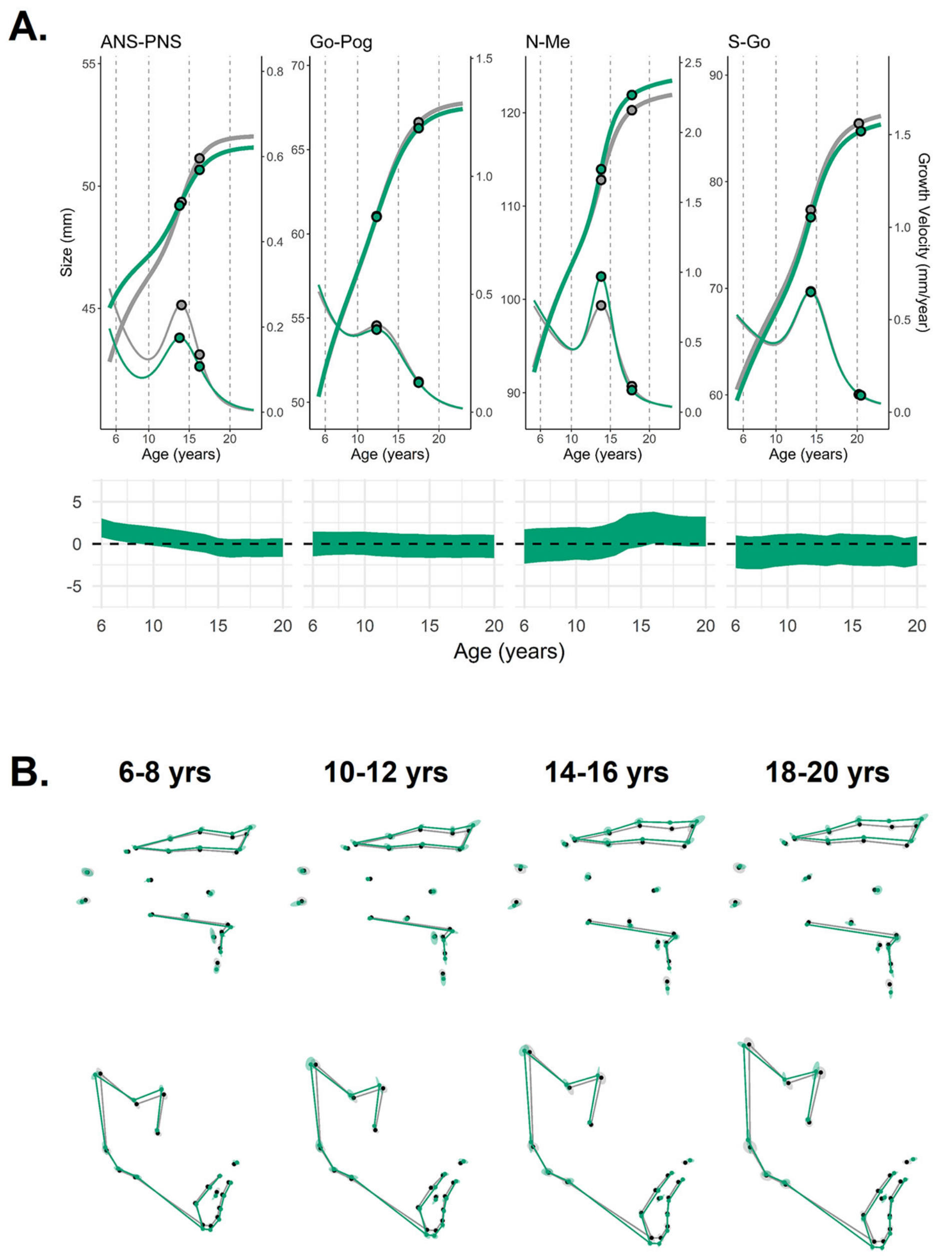

Figure 3:

Comparison of hyper-divergent Class I growth (solid green lines) to normo-divergent Class I growth (solid gray lines) in males. A: Plots for each of the four measurements with a double-logistic growth curve and velocity curve for each classification group. Below each plot shows the HPDI comparing distribution values between classification groups. B: Comparison of cranial and mandibular morphology between the two classification groups at the four timepoints.

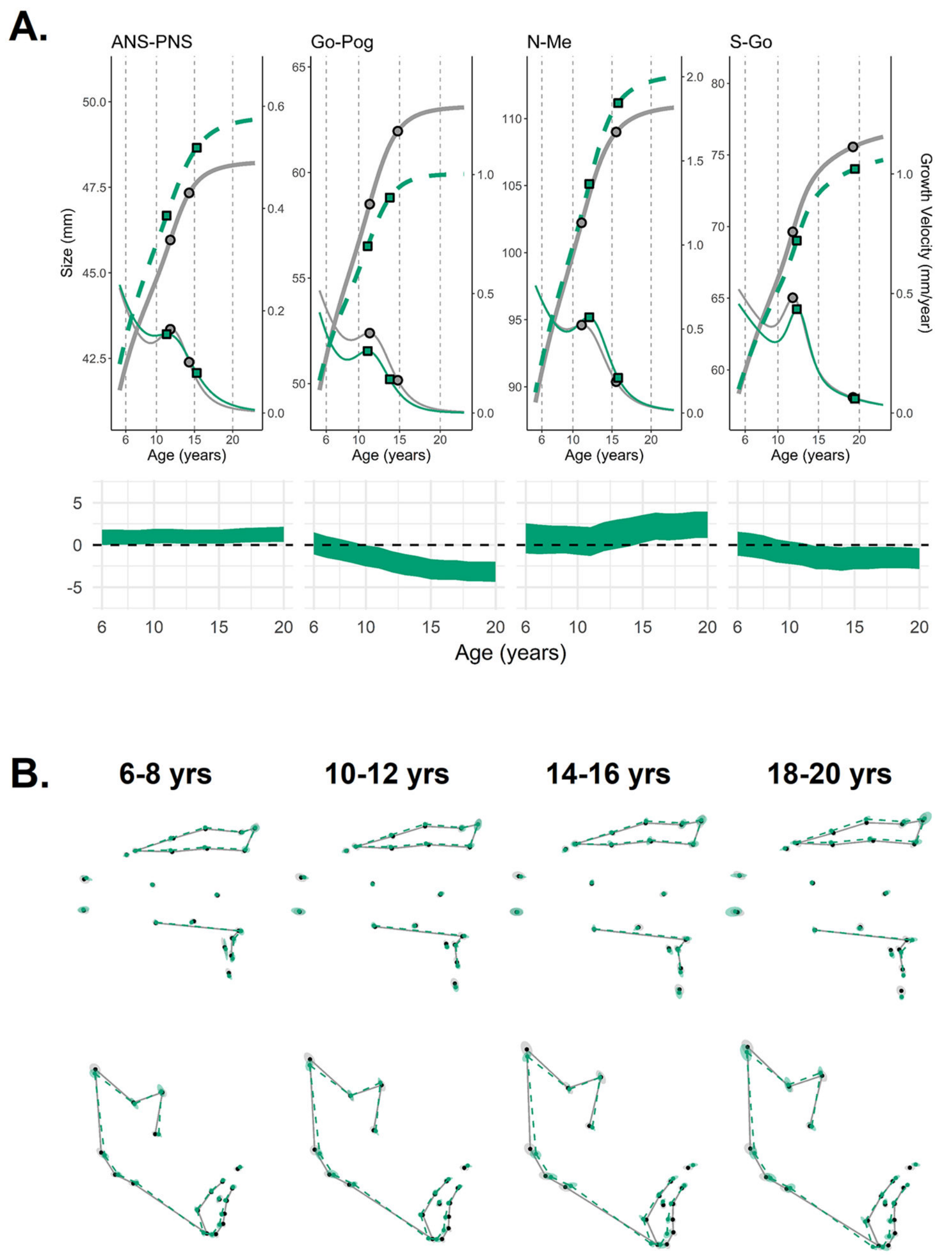

Figure 4:
Comparison of hyper-divergent Class II growth (dashed green lines) to normo-divergent Class I growth (solid gray lines) in females. A: Plots for each of the four measurements with a double-logistic growth curve and velocity curve for each classification group. Below each plot shows the HPDI comparing distribution values between classification groups. B: Comparison of cranial and mandibular morphology between the two classification groups at the four timepoints.

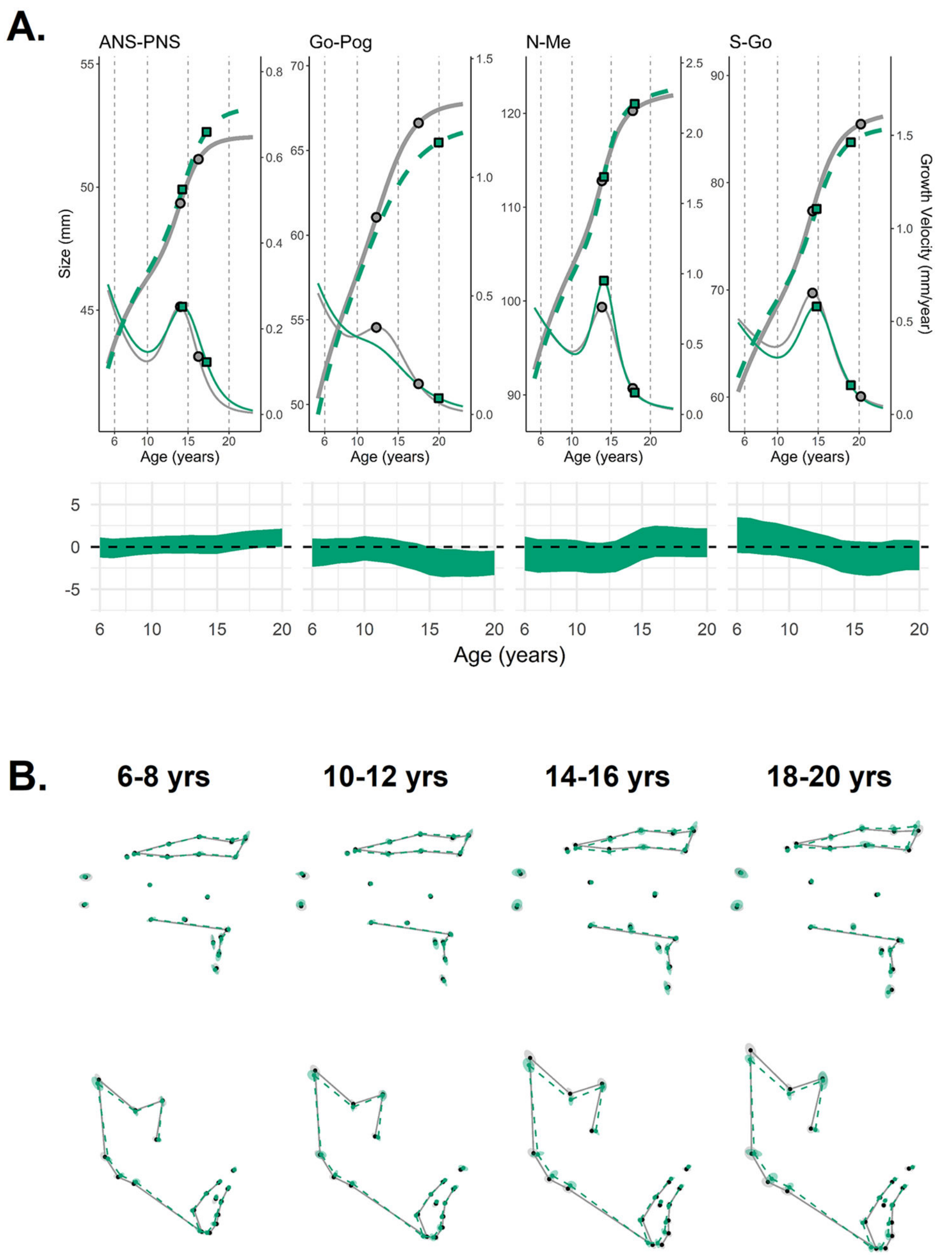

Figure 5:

Comparison of hyper-divergent Class II growth (dashed green lines) to normo-divergent Class I growth (solid gray lines) in males. A: Plots for each of the four measurements with a double-logistic growth curve and velocity curve for each classification group. Below each plot shows the HPDI comparing distribution values between classification groups. B: Comparison of cranial and mandibular morphology between the two classification groups at the four timepoints.

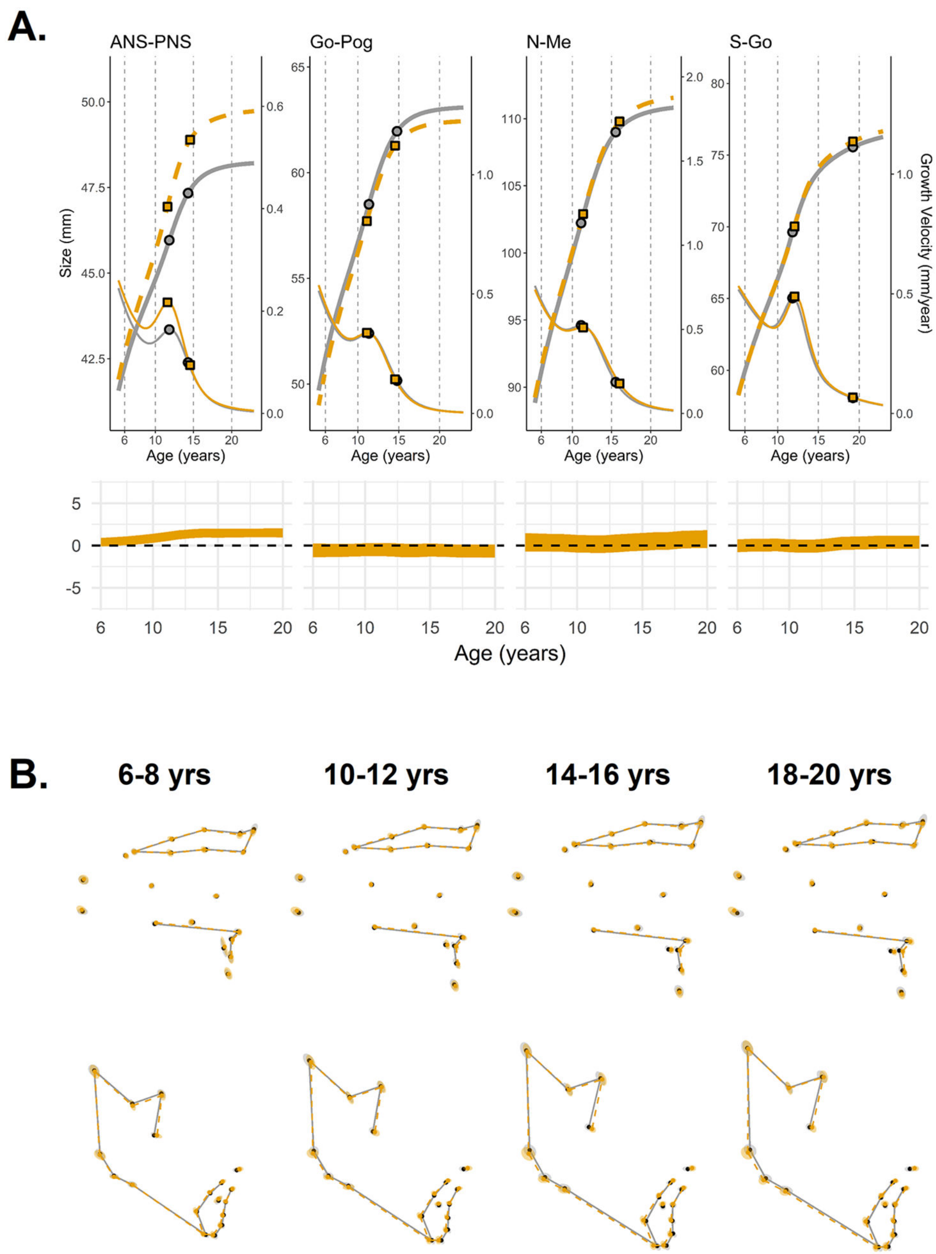

Figure 6:
Comparison of normo-divergent Class II growth (dashed yellow lines) to normo-divergent Class I growth (solid gray lines) in females. A: Plots for each of the four measurements with a double-logistic growth curve and velocity curve for each classification group. Below each plot shows the HPDI comparing distribution values between classification groups. B: Comparison of cranial and mandibular morphology between the two classification groups at the four timepoints.

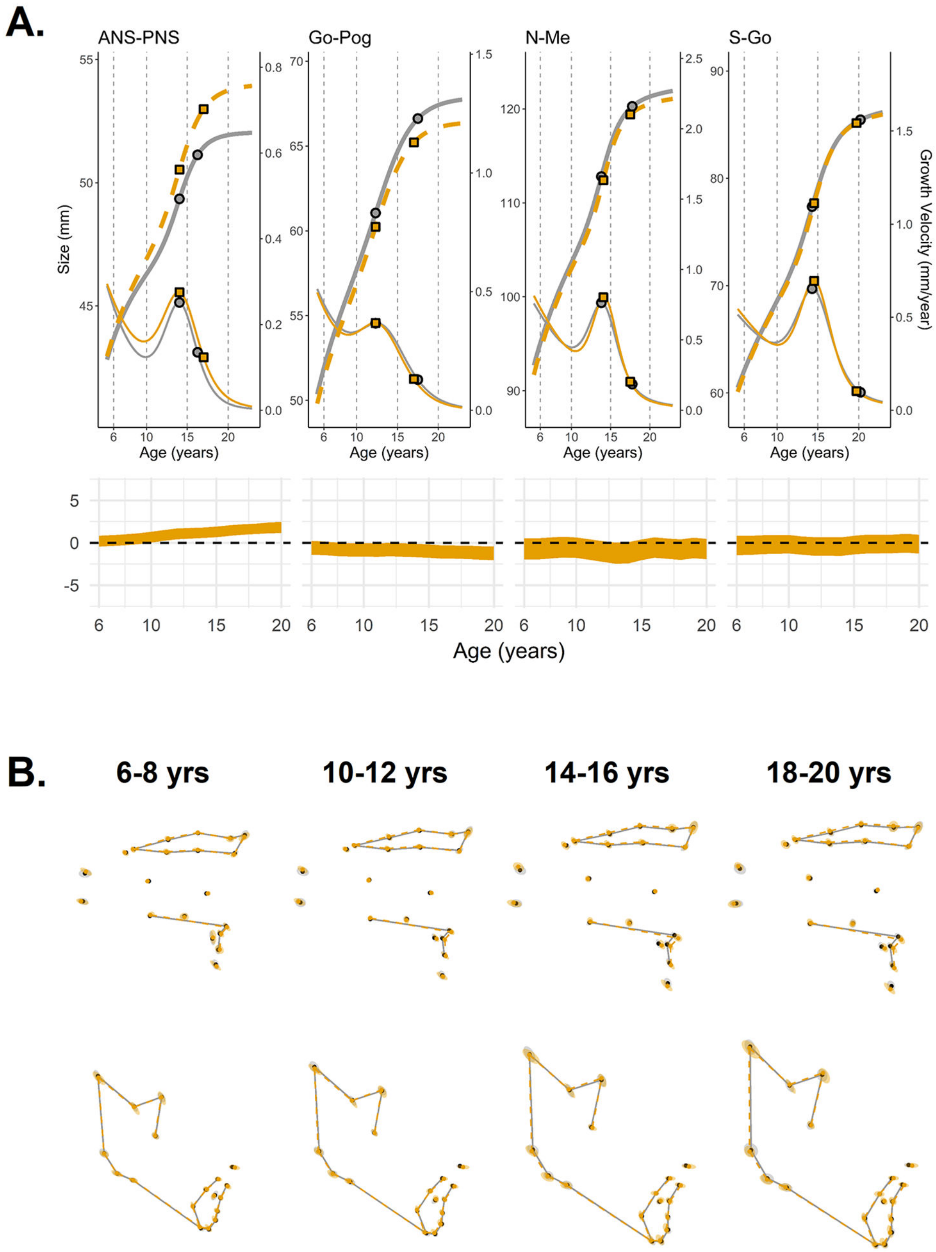

Figure 7:
Comparison of normo-divergent Class II growth (dashed yellow lines) to normo-divergent Class I growth (solid gray lines) in males. A: Plots for each of the four measurements with a double-logistic growth curve and velocity curve for each classification group. Below each plot shows the HPDI comparing distribution values between classification groups. B: Comparison of cranial and mandibular morphology between the two classification groups at the four timepoints.

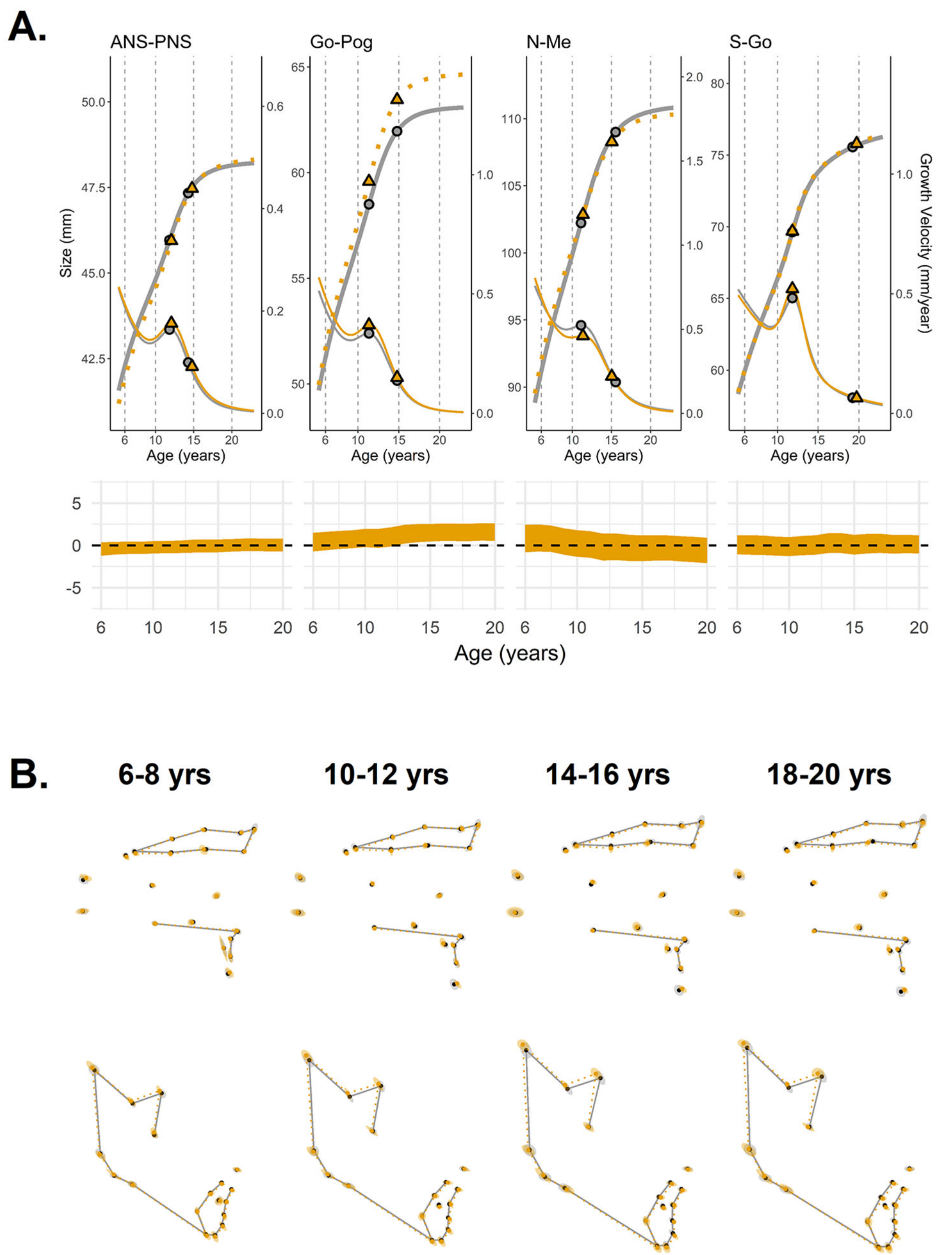

Figure 8:

Comparison of normo-divergent Class III growth (dotted yellow lines) to normo-divergent Class I growth (solid gray lines) in females. A: Plots for each of the four measurements with a double-logistic growth curve and velocity curve for each classification group. Below each plot shows the HPDI comparing distribution values between classification groups. B: Comparison of cranial and mandibular morphology between the two classification groups at the four timepoints.

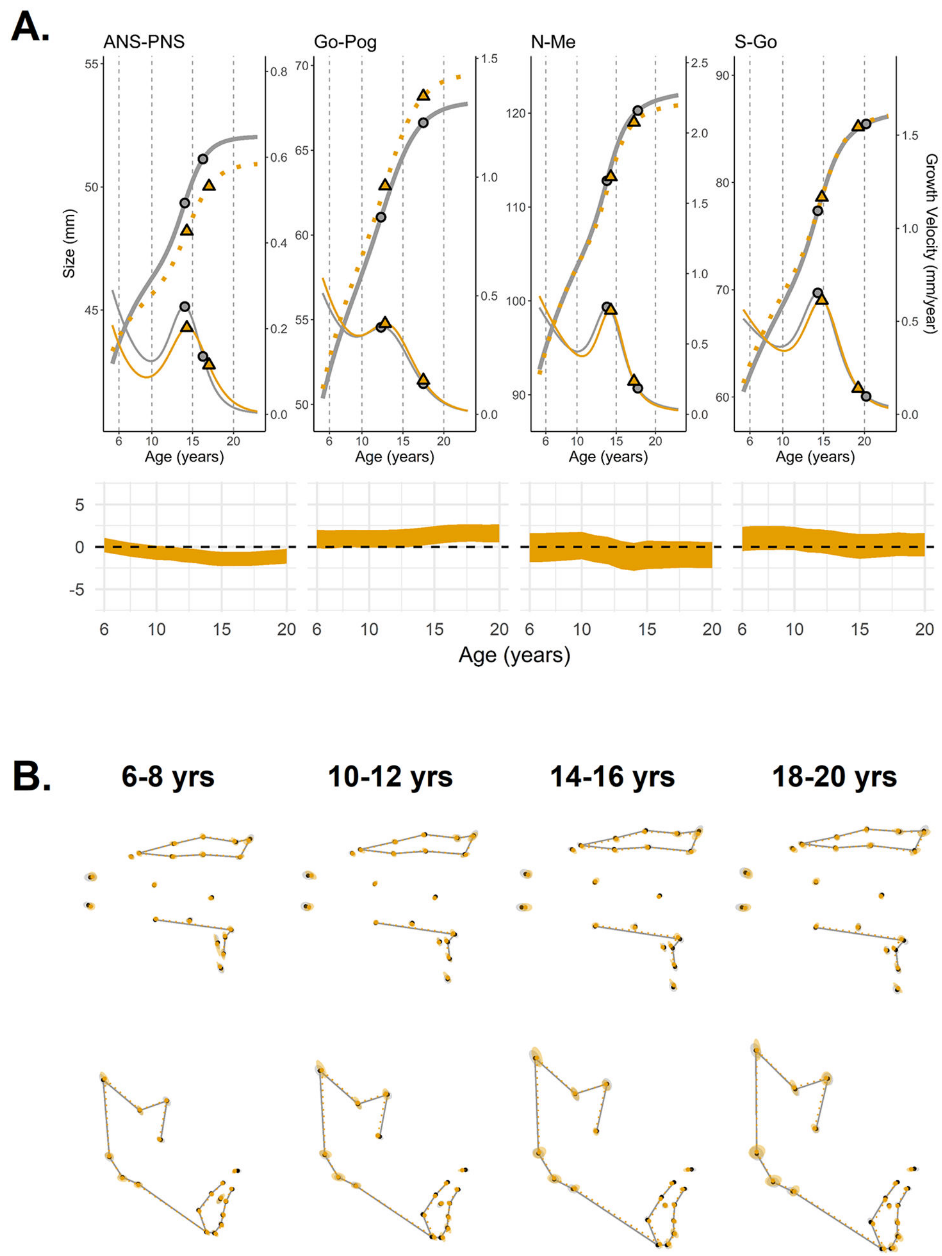

Figure 9:
Comparison of normo-divergent Class III growth (dotted yellow lines) to normo-divergent Class I growth (solid gray lines) in males. A: Plots for each of the four measurements with a double-logistic growth curve and velocity curve for each classification group. Below each plot shows the HPDI comparing distribution values between classification groups. B: Comparison of cranial and mandibular morphology between the two classification groups at the four timepoints.

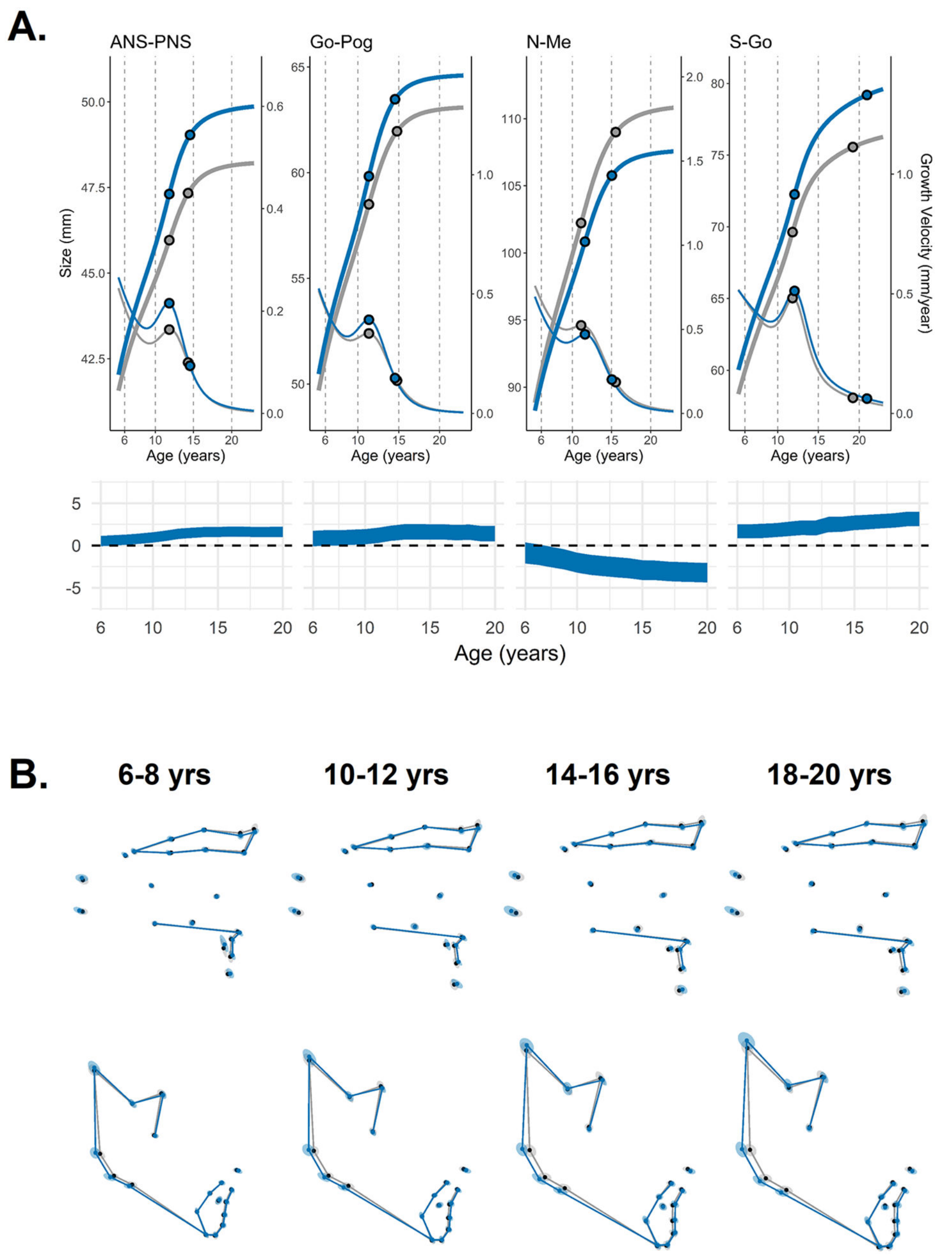

Figure 10:

Comparison of hypo-divergent Class I growth (solid blue lines) to normo-divergent Class I growth (solid gray lines) in females. A: Plots for each of the four measurements with a double-logistic growth curve and velocity curve for each classification group. Below each plot shows the HPDI comparing distribution values between classification groups. B: Comparison of cranial and mandibular morphology between the two classification groups at the four timepoints.

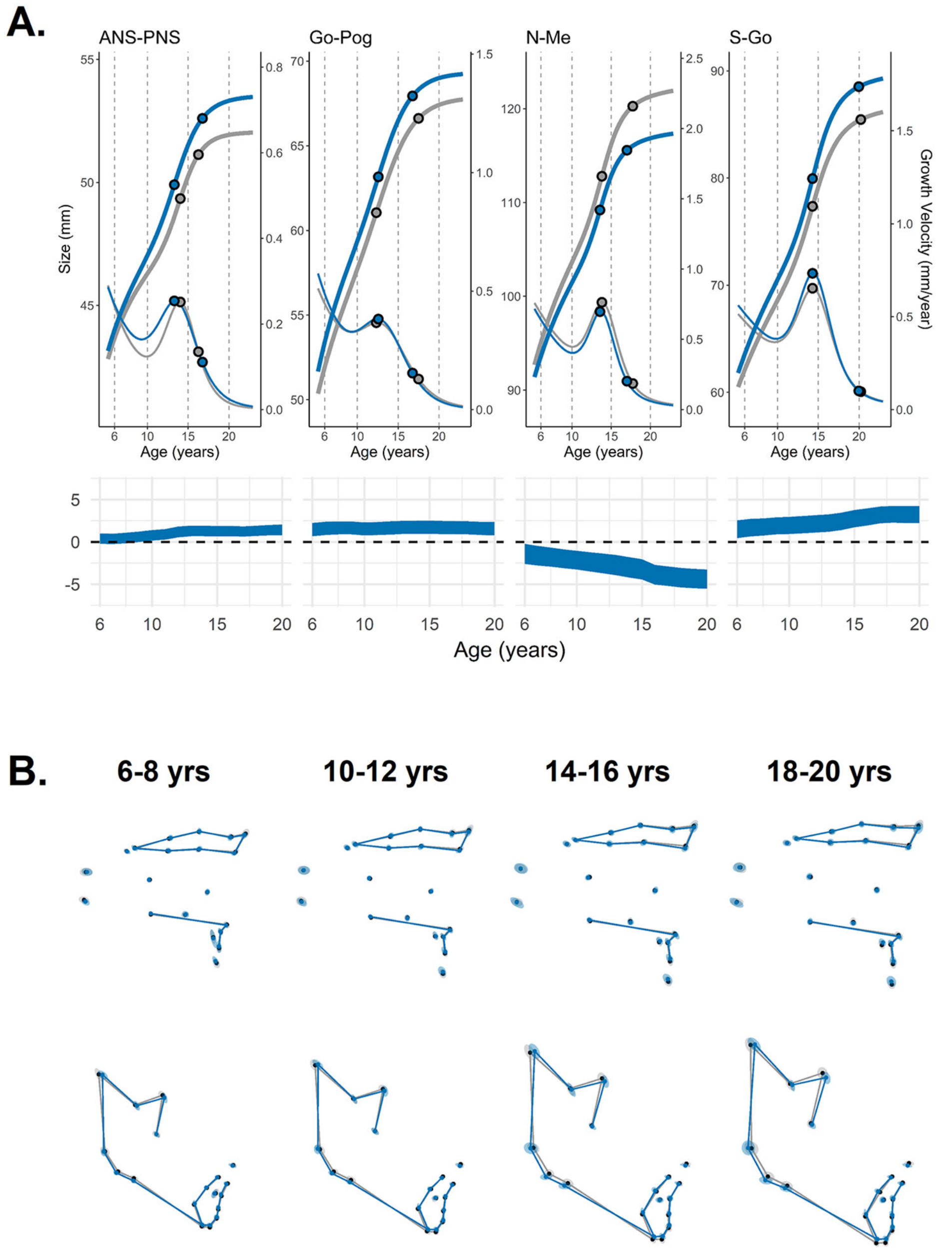

Figure 11:

Comparison of hypo-divergent Class I growth (solid blue lines) to normo-divergent Class I growth (solid gray lines) in males. A: Plots for each of the four measurements with a double-logistic growth curve and velocity curve for each classification group. Below each plot shows the HPDI comparing distribution values between classification groups. B: Comparison of cranial and mandibular morphology between the two classification groups at the four timepoints.

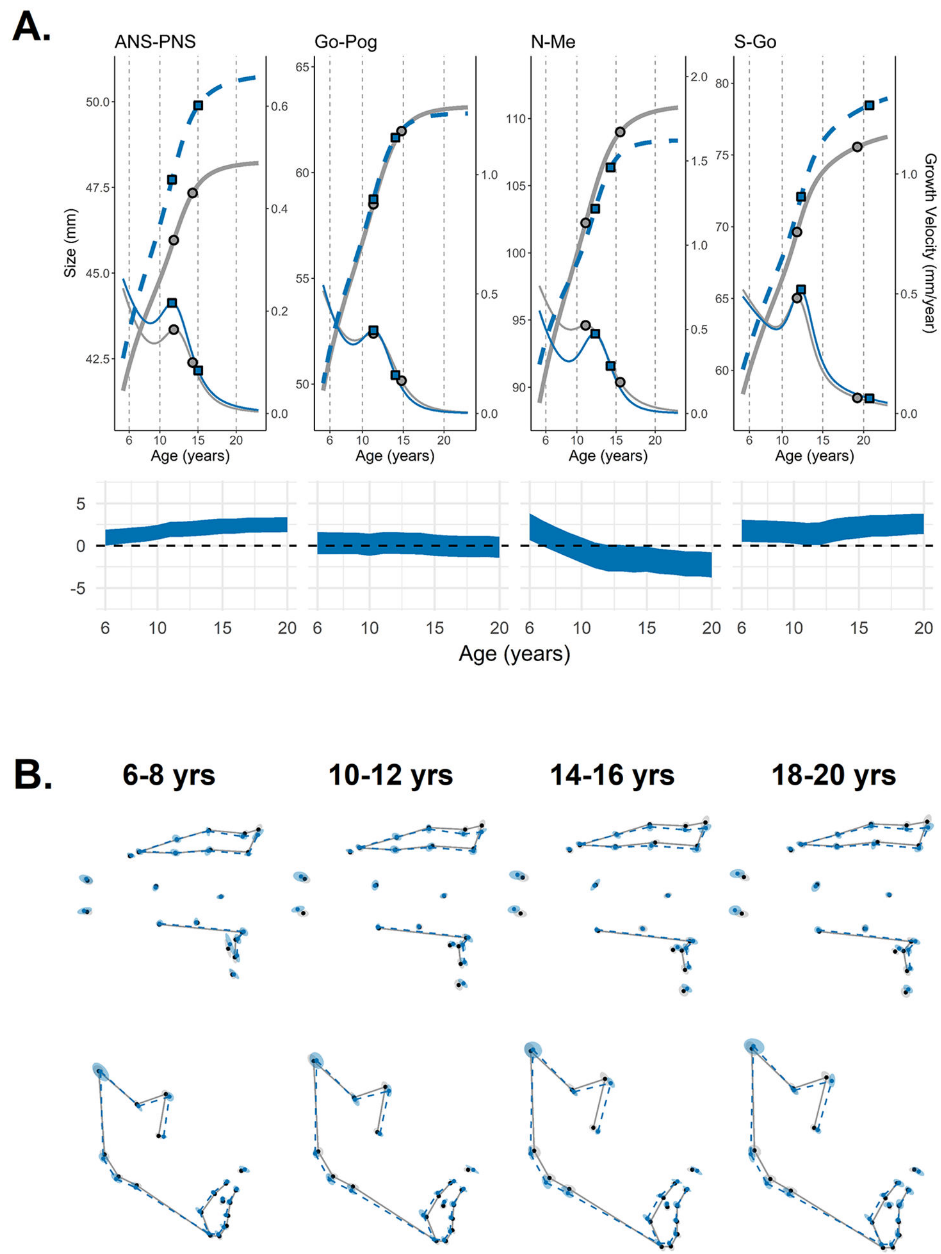

Figure 12:
Comparison of hypo-divergent Class II growth (dashed blue lines) to normo-divergent Class I growth (solid gray lines) in females. A: Plots for each of the four measurements with a double-logistic growth curve and velocity curve for each classification group. Below each plot shows the HPDI comparing distribution values between classification groups. B: Comparison of cranial and mandibular morphology between the two classification groups at the four timepoints.

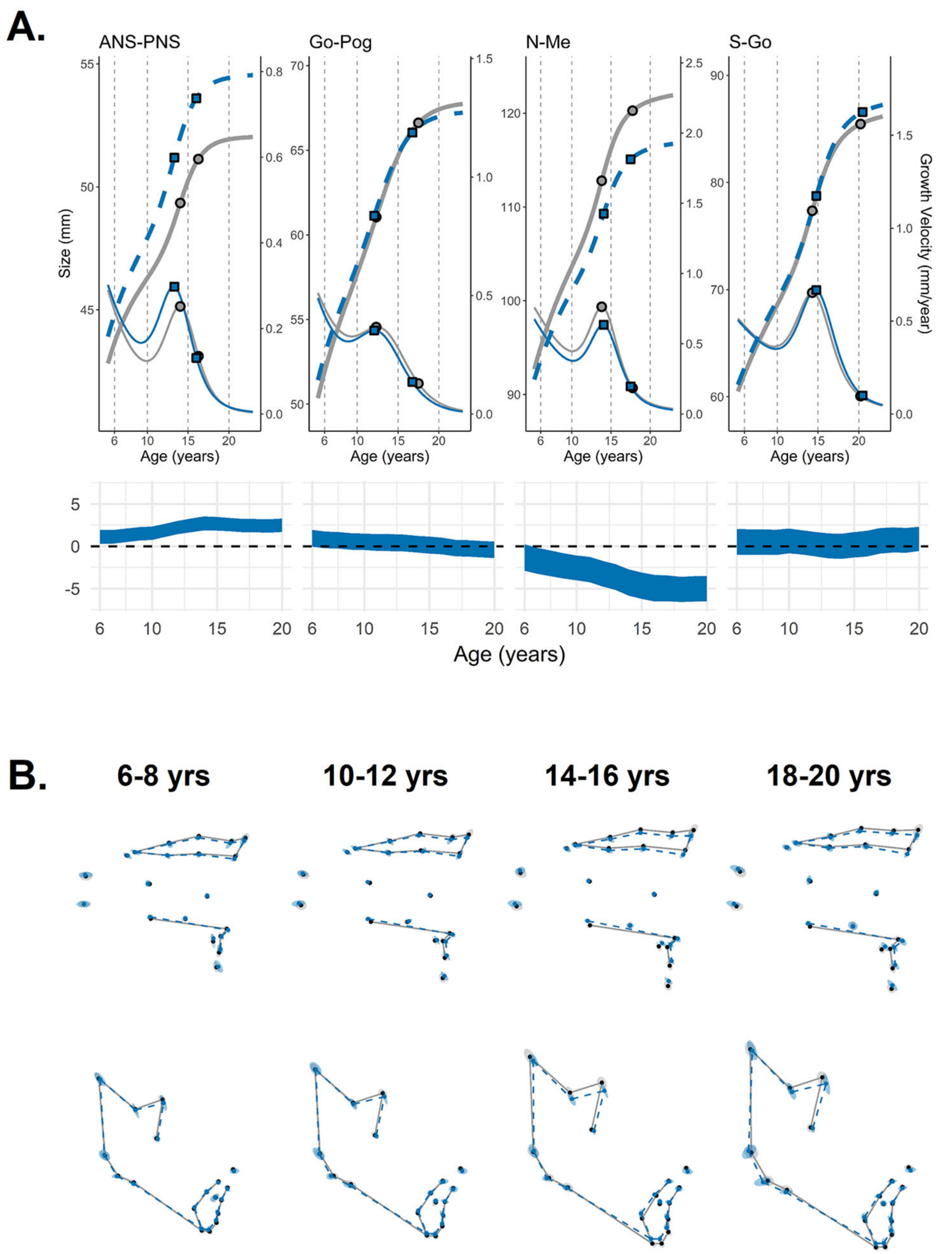

Figure 13:
Comparison of hypo-divergent Class II growth (dashed blue lines) to normo-divergent Class I growth (solid gray lines) in males. A: Plots for each of the four measurements with a double-logistic growth curve and velocity curve for each classification group. Below each plot shows the HPDI comparing distribution values between classification groups. B: Comparison of cranial and mandibular morphology between the two classification groups at the four timepoints.

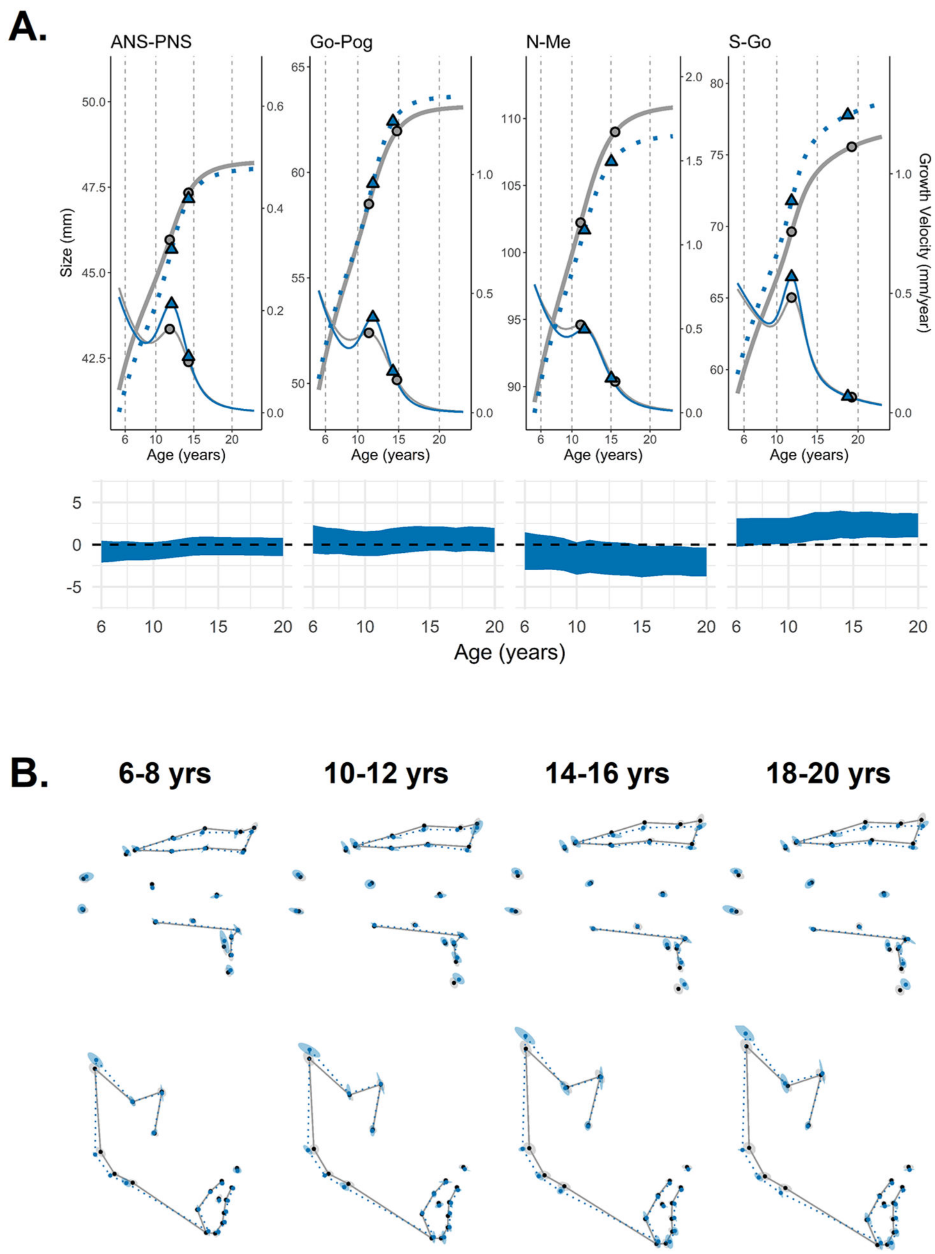

Figure 14:

Comparison of hypo-divergent Class III growth (dotted blue lines) to normo-divergent Class I growth (solid gray lines) in females. A: Plots for each of the four measurements with a double-logistic growth curve and velocity curve for each classification group. Below each plot shows the HPDI comparing distribution values between classification groups. B: Comparison of cranial and mandibular morphology between the two classification groups at the four timepoints.

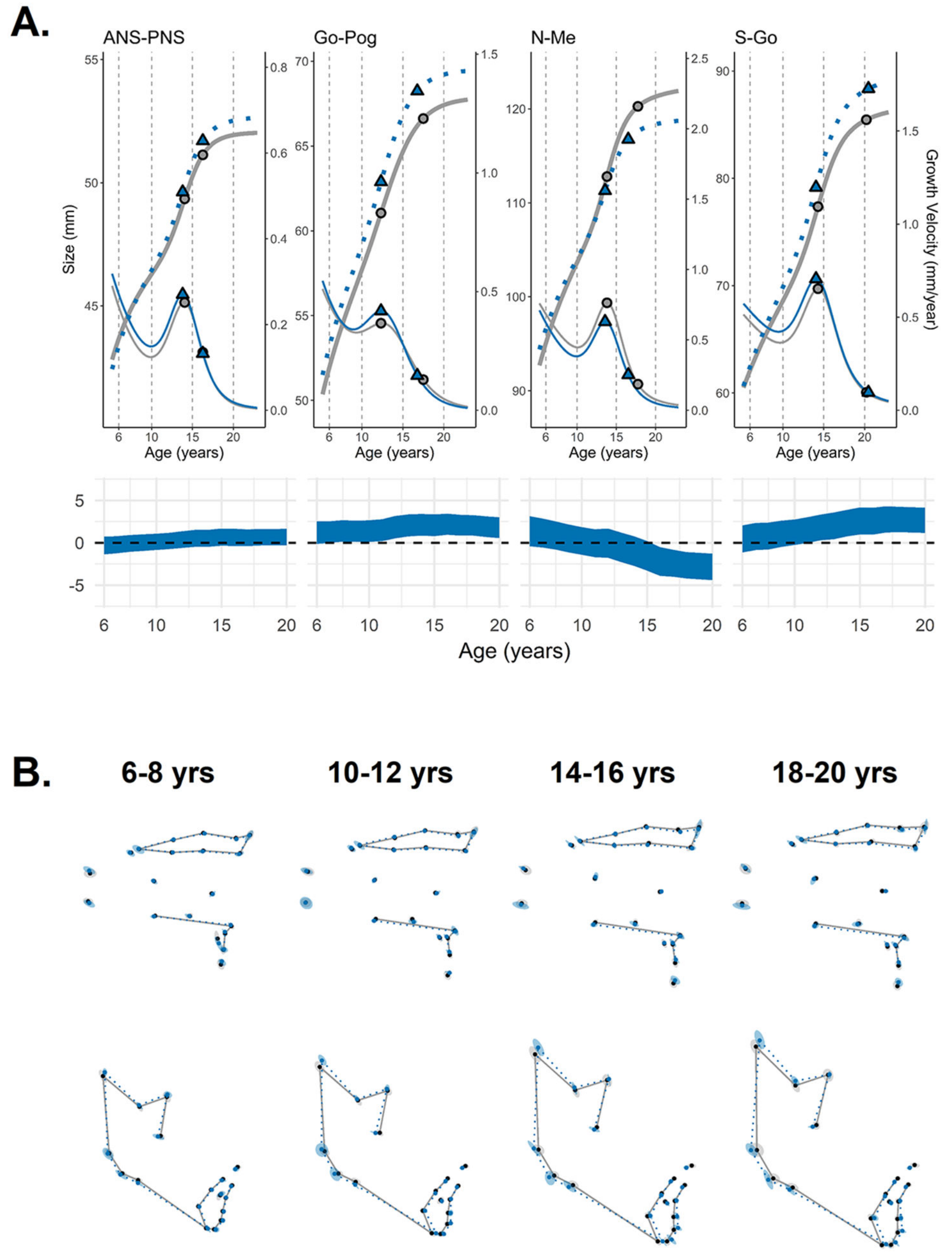

Figure 15:

Comparison of hypo-divergent Class III growth (dotted blue lines) to normo-divergent Class I growth (solid gray lines) in males. A: Plots for each of the four measurements with a double-logistic growth curve and velocity curve for each classification group. Below each plot shows the HPDI comparing distribution values between classification groups. B: Comparison of cranial and mandibular morphology between the two classification groups at the four timepoints.

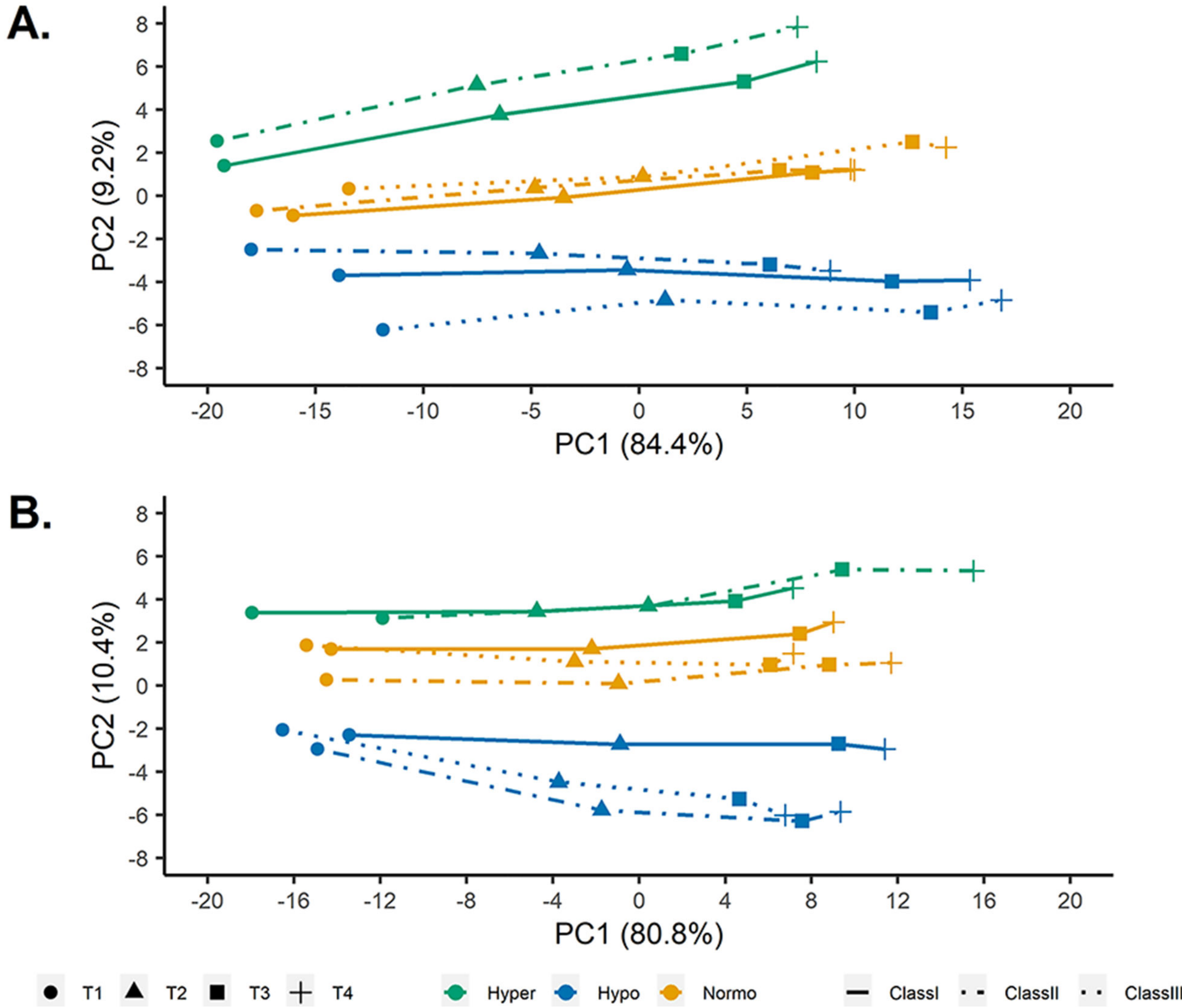

Figure 16:

PC1 and PC2 of principal component analyses of mean mandibular (A) and cranial (B) landmark configurations for each type-class group at each timepoint in females.

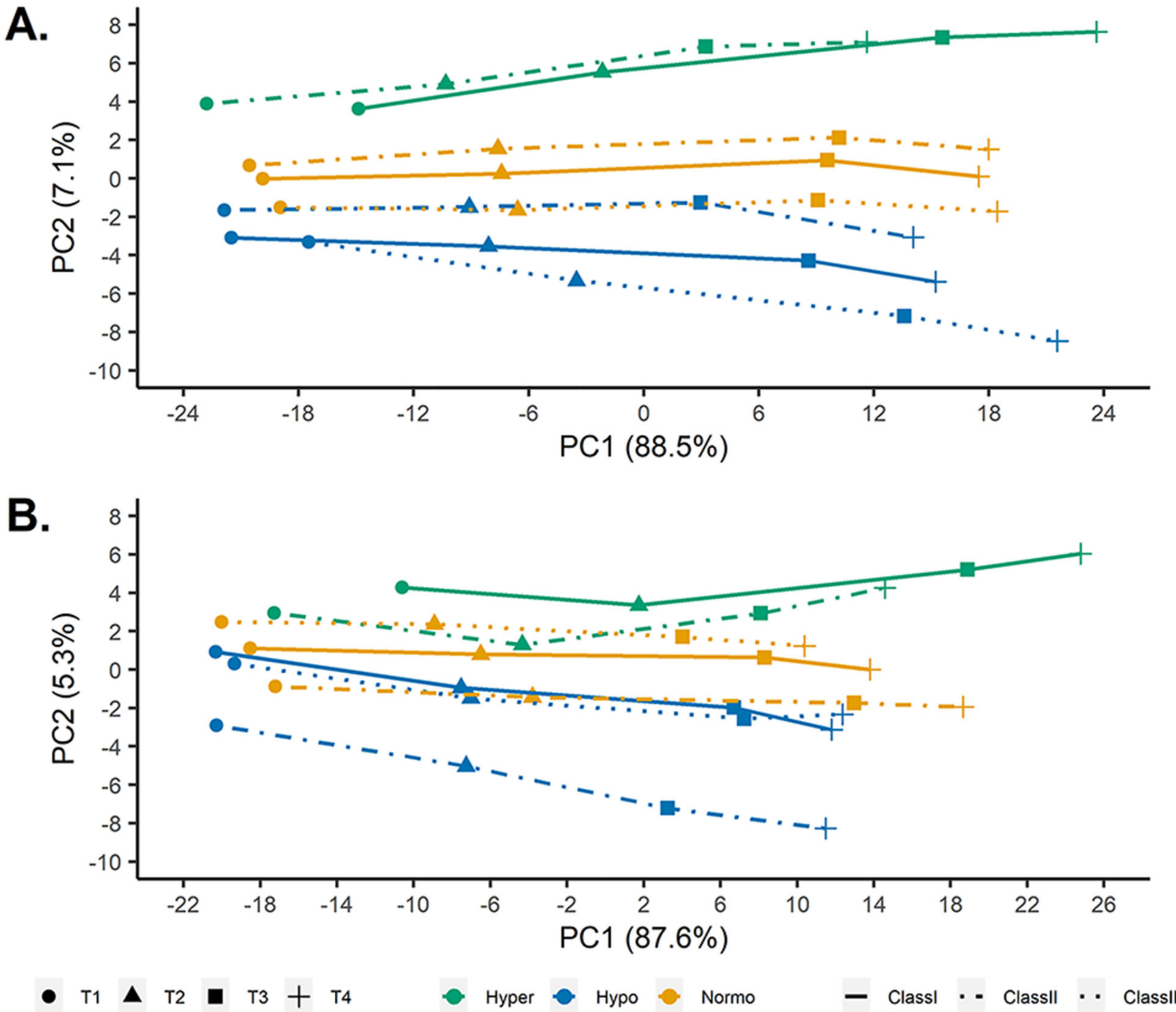

Figure 17:
PC1 and PC2 of principal component analyses of mean mandibular (A) and cranial (B) landmark configurations for each type-class group at each timepoint in males.

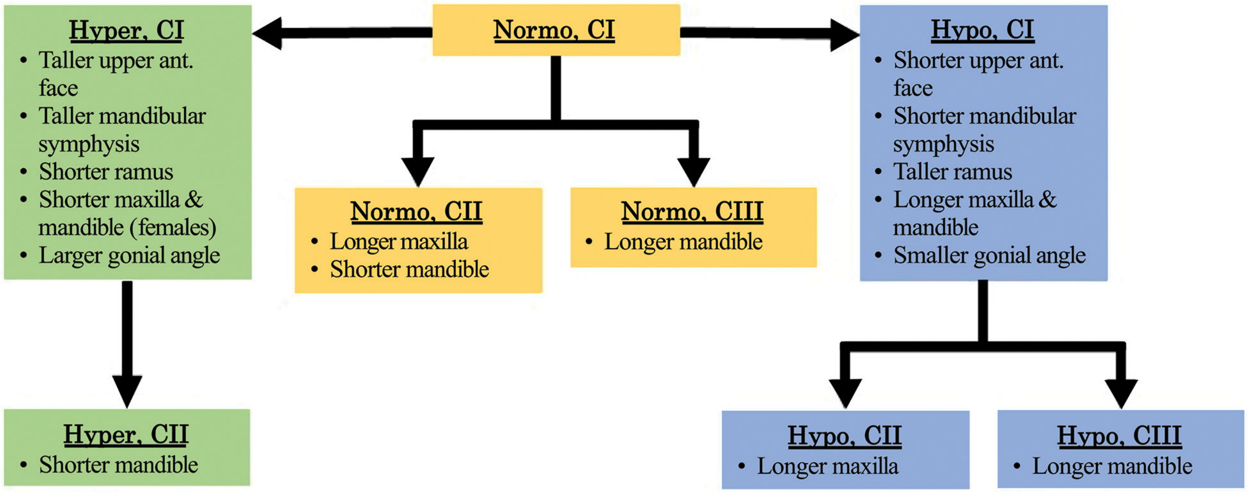

Figure 18:

Summary of morphological patterns observed among different craniofacial classifications in this study.

Table 1.

Description of landmarks collected for this study.

CRANIUM		
Number	**Name**	**Definition**
1	SELLA	Mid-point of the pituitary fossa
2	NASION	Most antero-inferior point on the frontal bone at the naso-frontal suture
3	ORBITALE	Inferior-most point of the orbital margin of the more anterior orbital image
4	U I APEX	Point of intersection between the long axis of the more anteriorly positioned upper central incisor and the contour of that tooth's root-end curvature
5	POINT A	Deepest point on the curvature of the surface of the maxillary bone between ANS and the alveolar crest of the upper central incisor
6	U I EDGE	Tip of the incisal edge of the more anteriorly placed upper central incisor
7	PNS	Intersection between the posterior extension of the superior surface of the palate and the downward extension of the pterygomaxillary fissure
8	BASION	Inferior-most point on the anterior margin of the foramen magnum in the midsagittal plane
9	PORION	Most superior point of the external auditory meatus of the right ear
10	ANS	Anterior-most point of the anatomical anterior nasal spine
11	GLABELLA	Most anterior point on the osseous forehead
12	SE	Midpoint between the intersections of the two great wings of the sphenoid bone with the sphenoid plane
13	POINT P	Point of greatest convexity between the anterior contour of sella turcica and the sphenoid plane
14	PTM	Pterygomaxillary fissure point: intersection of the inferior border of the foramen rotundum with the posterior wall of the pterygomaxillary fissure
15	PROSTHION	Most inferior and anterior point of the maxillary alveolar process
16	FRONT	Point of intersection between the roof of orbit line and the *internal* cortical plate of the frontal bone
17	ROOF	Most superior point of the roof of orbit, middle point between FRONT and SE-S
18	SE-S	Point of intersection of the greater wing of the sphenoid bone and the roof of orbit (midpoint between two greater wings of the sphenoid bone)
19	ETHMOID	Point of intersection between the lateral border of the ethmoid bone and the vertical extension of the most anteriorly positioned Key ridge
20	ZYGOMA	Most inferior point of the most anteriorly positioned Key ridge
MANDIBLE		
21	L I EDGE	Tip of the incisal edge of the more anteriorly placed lower central incisor
22	POINT B	Deepest point on the curvature of the anterior border of the mandible between pogonion and the alveolar crest of the lower central incisor
23	L I APEX	Point of intersection between the long axis of the most anteriorly positioned lower incisor and the contour of that tooth's root-end curvature.
24	POGONION	Anterior-most point of the bony chin at the midline
25	MENTON	Inferior-most point on the mandible at the symphysis
26	CONDYLE	Point on the posterior-superior contour of the condyle that is the longest distance from pogonion
27	SIGMOID	Deepest point of the sigmoid notch
28	P RAMUS	Posterior ramus point where the inflection starts
29	CORONOID	Tip of the coronoid process
30	A RAMUS	Deepest point in the anterior ramus

CRANIUM		
Number	**Name**	**Definition**
31	INFRADENTALE	Most superior and anterior point of the mandibular alveolar process
32	LINGUAL L1	Most superior and anterior point of alveolar bone on the lingual surface
33	LINGUAL POINT B	Intersecting point of a posterior extension of point B parallel to the mandibular plane connecting gonion and menton on the lingual cortical plate of the symphysis
34	PROMENTI	Protuberance menti (suprapogonion)-the point where the shape of the symphysis mentalis changes from convex to concave
35	L_SYMPHY	Intersecting point of a posterior extension of pogonion parallel to the mandibular plane connecting gonion and menton on the lingual cortical plate of the symphysis
36	GNATHION	Point located by taking the midpoint between pogonion and menton of the bony chin
37	ANTEGONION	Deepest point of the antegonial notch
38	GONION	Average of upper and lower gonion points

Table 2.

Number of individuals in each facial category, by sex, used in traditional cephalometric and geometric morphometric analyses.

		Bayesian longitudinal analysis		GMM analysis	
MPA Type	**ANB Class**	**Females**	**Males**	**Females**	**Males**
Hyper-divergent	Class I	18	12	7	6
	Class II	17	12	9	8
Normo-divergent	Class I	104	102	56	51
	Class II	83	61	43	23
	Class III	25	24	11	17
Hypo-divergent	Class I	54	69	30	31
	Class II	17	29	11	11
	Class III	8	17	4	6
Total		**326**	**326**	**168**	**159**

Table 3.

Summary of growth parameters including age at peak growth velocity (aPGV), peak growth velocity (PGV), and age at growth cessation (aGC). Comparisons were made for each classification category (e.g., Hyper-divergent Class I) in comparison to the control group (i.e., Normo-divergent Class I) for each measurement and separately by sex. = denotes less than a 6 month age difference or less than a 0.05 mm/year difference in growth velocity. ↓ denotes earlier age or slower growth compared to the control group. ↑ denotes older age or faster growth compared to the control group.

			ANS-PNS			Go-Pog			N-M			S-Go		
			aPGV	PGV	aGC	aPGV	PGV	aGC	aPGV	PGV	aGC	aPGV	PGV	aGC
Females	Hyper-divergent	Class I	=	=	=	=	=	↓	=	↑	=	=	↓	↑
		Class II	=	=	↑	=	↓	↓	↑	=	=	=	=	=
	Normo-divergent	Class II	=	↑	=	=	=	=	=	=	=	=	=	=
		Class III	=	=	=	=	=	=	=	↓	=	=	=	=
	Hypo-divergent	Class I	=	↑	=	=	↑	=	=	↓	=	=	=	↑
		Class II	=	↑	↑	=	=	↓	↑	↓	↓	=	=	↑
		Class III	=	↑	=	=	↑	=	=	=	=	=	↑	=

			ANS-PNS			Go-Pog			N-Me			S-Go		
			aPGV	PGV	aGC	aPGV	PGV	aGC	aPGV	PGV	aGC	aPGV	PGV	aGC
Males	Hyper-divergent	Class I	=	↓	=	=	=	=	=	↑	=	=	=	=
		Class II	=	=	↑	NA	NA	↑	=	↑	=	=	↓	↓
	Normo-divergent	Class II	=	=	↑	=	=	=	=	=	=	=	=	=
		Class III	=	↓	↑	=	=	=	=	=	=	=	=	↓
	Hypo-divergent	Class I	↓	=	=	=	=	↓	=	↓	↓	=	↑	=
		Class II	↓	=	=	=	=	↓	=	↓	=	=	=	=
		Class III	=	=	=	=	↑	↓	=	↓	↓	=	↑	=